

Neutrino Phenomenology and Dark matter in an A_4 flavour extended $B - L$ model

Subhasmita Mishra^a, Mitesh Kumar Behera^b, Rukmani Mohanta^b,
Sudhanwa Patra^c, Shivaramakrishna Singirala^d

^aDepartment of Physics, IIT Hyderabad, Kandi - 502285, India

^bSchool of Physics, University of Hyderabad, Hyderabad - 500046, India

^cIndian Institute of Technology Bhilai, GEC Campus, Sejbahar, Raipur-492015, India

^dDiscipline of Physics, Indian Institute of Technology Indore, Indore-453 552, India

E-mail: subhasmita.mishra92@gmail.com, miteshbehera1304@gmail.com,
rmsp@uohyd.ac.in, sudhanwa@iitbhillai.ac.in, krishnas542@gmail.com

Abstract. We present an A_4 flavor extended $B - L$ model for realization of eV scale sterile neutrinos, motivated by the recent experimental hints from both particle physics and cosmology. The framework considered here is a gauged $B - L$ extension of standard model without the introduction of right-handed neutrinos, where the gauge triangle anomalies are canceled with the inclusion of three exotic neutral fermions N_i ($i = 1, 2, 3$) with $B - L$ charges $-4, -4$ and 5 . The usual Dirac Yukawa couplings between the SM neutrinos and the exotic fermions are absent and thus, the model allows natural realization of eV scale sterile-like neutrino and its mixing with standard model neutrinos by invoking A_4 flavor symmetry. We demonstrate how the exact tri-bimaximal mixing pattern is perturbed due to active-sterile mixing by analyzing $3 + 1$ case in detail. We also show the implication of eV scale sterile-like neutrino on various observables in neutrino oscillation experiments and the effective mass in neutrinoless double beta decay. Another interesting feature of the model is that one of three exotic fermions is required to explain eV scale phenomena, while the lightest fermion mass eigenstate of the other two is a stable dark matter candidate. We constrain the gauge parameters associated with $U(1)$ gauge extension, using relic density and collider bounds.

Keywords: A_4 flavour symmetry, Sterile Neutrino, Dark Matter

Contents

1	Introduction	1
2	Model Description	3
2.1	Scalar potential and symmetry breaking pattern	4
2.2	CP-odd and CP-even scalar mass matrices	4
2.3	Lagrangian and Leptonic Mass matrix	5
3	Neutrino mixing with one sterile-like neutrino	6
3.1	Diagonalization of Neutrino Mass matrix	7
3.2	Numerical Analysis	10
3.2.1	Variation of model parameters by fixing $\lambda_2 = 1$ and $\phi_{ba} = 0$	11
3.2.2	Variation of model parameters by fixing $\lambda_2 = 1$ and $\phi_{ba} \neq 0$	14
4	Discussion on neutrinoless double beta decay with eV-scale neutrinos.	15
5	Dark Matter Phenomenology	20
6	Summary and Conclusion	22
7	Acknowledgment	23

1 Introduction

Albeit its success, Standard Model (SM) is not the complete theory of nature to explain many observed phenomena. Neutrino oscillation experiments, in contrast to the zero mass prediction of SM, have confirmed the need for massive neutrinos and thus, necessitates for physics beyond the SM (BSM). The massive neutrinos and most of neutrino oscillation data can be explained in a framework of three active neutrinos through the elegant canonical see-saw mechanism [1–6], whereas some experimental observations are strongly hinting towards one or two additional light neutrinos with eV scale masses and $\mathcal{O}(0.1)$ mixing with active neutrinos [7–11], stemming from particle physics, cosmology and astrophysics (for details, reader may refer to the white paper [12]). While large number of experiments are coming up in next few years in order to investigate the possible presence of eV scale sterile neutrinos, which would be a ground-breaking discovery, there are few model building efforts in this direction. The aim of this work is to provide a simple BSM framework explaining the presence of one eV scale sterile neutrino along with $\mathcal{O}(0.1)$ mixing with active neutrinos and their effects on neutrinoless double beta decay (NDBD). This model also provides a detail study of DM phenomenology via a TeV scale fermionic DM and the collider constraints from Z' mass.

The smallness of neutrino mass and their hierarchical structure become one of the most challenging problems in particle physics. In the standard scenario of three active neutrino oscillation, two mass-squared differences of order 10^{-5} eV^2 and 10^{-3} eV^2 , are observed from solar and atmospheric neutrino oscillation experiments respectively [13]. In fact, the absolute scale of neutrino mass still remains as an open question to be solved, however, there exists an upper bound on the sum of active neutrino masses, $\sum m_\nu < 0.12 \text{ eV}$ from cosmological observations [14]. Over the last two decades, several dedicated experiments have determined the neutrino oscillation parameters rather precisely, though few of them are still unknown. These include the neutrino mass ordering, the exact domain of the atmospheric mixing angle θ_{23} (octant problem) and the CP violating phase δ_{CP} . But there exist few experimental anomalies, which can not be explained within the standard three neutrino framework. Of them, one is the possible presence of sterile neutrinos [15], which is evident from the anti-neutrino flux measurement in LSND [12] and MiniBooNE [16] experiments. The excess flux of $\bar{\nu}_e$ in appearance mode during $\nu_\mu \rightarrow \nu_e$ oscillation, hints towards the possible existence of at least one additional state with eV scale mass [17]. This new state should not have any gauge interaction as per the Z -boson precision measurement and hence being sterile in nature. Thus, theoretical explanation of eV scale sterile neutrinos and its order of 0.1 mixing with the active neutrinos is worth to study through possible BSM frameworks. The non-trivial mixing of such a light sterile neutrino with SM neutrinos are well studied in the literature within different seesaw framework [18–26]. Along with these issues, the nature of neutrinos, i.e., whether it is Dirac or Majorana also remains unexplained. The only way to test the Majorana nature of neutrinos is through the extremely rare lepton-number violating neutrino-less double beta decay (NDBD) experiments.

One more well-known challenging problem in particle cosmology is that, SM doesn't have any explanation about the existence of DM even though we have enough indirect gravitational evidence about its existence. Attempts have been made through DM getting scattered off the SM particles i.e., in the context of direct searches, and the well known collaborations include LUX, XENON, PICO, PandaX etc [27, 28]. Study of excess in positron, electron or Gamma excess i.e., indirect signals, and the experiments include AMS-02, H.E.S.S, MAGIC, Fermi-LAT etc [29–33]. Apart from these, dark sector particle production is also probed in the accelerator experiments as well.

To explain these experimental discrepancies, SM needs to be extended with extra symmetries or particles. Discrete symmetries are mostly preferred by the phenomenologists for model building purpose as they restrict the interaction terms by giving a specific structure to the mass matrix. A_4 flavor symmetry is widely used in neutrino phenomenology as it gives the simple tribimaximal (TBM) mixing, which is more or less compatible with the standard neutrino mixing matrix (U_{PMNS}). But this mixing pattern predicts a vanishing reactor mixing angle θ_{13} [34], which conflicts the current experimental observation. Myriad amount of literature is focused on neutrino phenomenology with A_4 symmetry in the frameworks of

different seesaw mechanism [34–39]. Apart from neutrino phenomenology, phenomenological study of DM has been made within A_4 framework [40–44], but very few literature have been devoted to study these phenomena with gauge extended A_4 flavor symmetric model. We consider a minimal extension of SM with A_4 and $U(1)_{B-L}$ symmetry in addition to three flavon fields and three singlet scalars, responsible for the breaking of A_4 and $U(1)_{B-L}$ symmetry respectively. This model includes three additional fermions with exotic $B - L$ charges of -4 , -4 , 5 to protect from triangle gauge anomalies. This extension enhances the predictability of the model by explaining different phenomenological consequences like DM, neutrino mass and NDBD, compatible with the current observations.

This manuscript is structured as: section 2 follows the brief description of model and particle content along with the full Lagrangian and symmetry breaking. In section 3, we discuss the neutrino masses and mixing with one sterile-like neutrino scenario and section 4 includes the contribution of active-sterile mixing to the NDBD as per current experimental observation. In section 5, we illustrate a detailed description of DM phenomenology and collider bounds on new gauge parameters within the model framework. In section 6, we summarize and conclude the phenomenological consequences of the model.

2 Model Description

We propose a new variant of $U(1)_{B-L}$ gauge extension of SM with additional A_4 flavor symmetry, which includes three new neutral fermions N_i 's ($i = 1, 2, 3$) with exotic $B - L$ charges -4 , -4 and $+5$ to nullify the triangle gauge anomalies [45]. This choice of adding three exotic fermions in the context of $B - L$ framework has been explored in several previous works [46–53]. The spontaneous symmetry breaking of $B - L$ gauge symmetry is realized with three singlet scalars (ϕ_2, ϕ_4 and ϕ_8), which also generate mass terms to all exotic fermions and the new gauge boson. Additionally, A_4 flavor symmetry is used to study the neutrino phenomenology in this model. Apart from the usual SM Higgs doublet and the above mentioned three scalar singlets, responsible for electroweak symmetry and $U(1)_{B-L}$ symmetry breaking respectively, there are three SM singlet flavon fields ϕ_T, χ, ζ to break the A_4 flavor symmetry.

In this work, we intend to provide a detailed description of oscillation phenomenology with one sterile-like neutrino scenario. The complete field content with their corresponding charges are provided in Tables 1 and 2. The multiplication rules under A_4 symmetry group is outlined in Appendix.

Field	L	e_R	μ_R	τ_R	H
$SU(2)_L$	2	1	1	1	2
A_4	3	1	$1''$	$1'$	1
$U(1)_{B-L}$	-1	-1	-1	-1	0

Table 1: SM field content of lepton and Higgs sectors alongwith their corresponding charges.

Field	N_1	N_2	N_3	ϕ_2	ϕ_4	ϕ_8	ϕ_T	χ	ζ
SU(2) _L	1	1	1	1	1	1	1	1	1
A ₄	1	1	1	1	1	1	3	3	1'
U(1) _{B-L}	5	-4	-4	2	4	8	-2	2	2

Table 2: Complete field content with their corresponding charges of the proposed model.

2.1 Scalar potential and symmetry breaking pattern

Considering all the scalar content of the model, the potential can be written as

$$\begin{aligned}
V = & \mu_H^2(H^\dagger H) + \lambda_H(H^\dagger H)^2 + \mu_2^2(\phi_2^\dagger \phi_2) + \lambda_{22}(\phi_2^\dagger \phi_2)^2 + \mu_4^2(\phi_4^\dagger \phi_4) + \lambda_4(\phi_4^\dagger \phi_4)^2 \\
& + \mu_8^2(\phi_8^\dagger \phi_8) + \lambda_8(\phi_8^\dagger \phi_8)^2 + \mu_T^2(\phi_T^\dagger \phi_T) + \lambda_T(\phi_T^\dagger \phi_T)^2 + \mu_\chi^2(\chi^\dagger \chi) + \lambda_\chi(\chi^\dagger \chi)^2 \\
& + \mu_\zeta^2(\zeta^\dagger \zeta) + \lambda_\zeta(\zeta^\dagger \zeta)^2 + \lambda_{H2}(H^\dagger H)(\phi_2^\dagger \phi_2) + \lambda_{H4}(H^\dagger H)(\phi_4^\dagger \phi_4) + \lambda_{H\chi}(H^\dagger H)(\chi^\dagger \chi) \\
& + \lambda_{H\zeta}(H^\dagger H)(\zeta^\dagger \zeta) + \lambda_{H8}(H^\dagger H)(\phi_8^\dagger \phi_8) + \lambda_{HT}(H^\dagger H)(\phi_T^\dagger \phi_T) + \lambda_{24}(\phi_2^\dagger \phi_2)(\phi_4^\dagger \phi_4) \\
& + \lambda_{28}(\phi_2^\dagger \phi_2)(\phi_8^\dagger \phi_8) + \lambda_{2T}(\phi_2^\dagger \phi_2)(\phi_T^\dagger \phi_T) + \lambda_{2\zeta}(\phi_2^\dagger \phi_2)(\zeta^\dagger \zeta) + \lambda_{2\chi}(\phi_2^\dagger \phi_2)(\chi^\dagger \chi) \\
& + \lambda_{48}(\phi_4^\dagger \phi_4)(\phi_8^\dagger \phi_8) + \lambda_{4T}(\phi_4^\dagger \phi_4)(\phi_T^\dagger \phi_T) + \lambda_{4\chi}(\phi_4^\dagger \phi_4)(\chi^\dagger \chi) + \lambda_{4\zeta}(\phi_4^\dagger \phi_4)(\zeta^\dagger \zeta) \\
& + \lambda_{8T}(\phi_8^\dagger \phi_8)(\phi_T^\dagger \phi_T) + \lambda_{8\chi}(\phi_8^\dagger \phi_8)(\chi^\dagger \chi) + \lambda_{8\zeta}(\phi_8^\dagger \phi_8)(\zeta^\dagger \zeta) + \lambda_{\chi T}(\chi^\dagger \chi)(\phi_T^\dagger \phi_T) \\
& + \lambda_{\chi\zeta}(\chi^\dagger \chi)(\zeta^\dagger \zeta) + \lambda_{\zeta T}(\zeta^\dagger \zeta)(\phi_T^\dagger \phi_T) + \mu_{24} \left((\phi_2)^2 \phi_4^\dagger + (\phi_2^\dagger)^2 \phi_4 \right) \\
& + \lambda_{248} \left((\phi_2)^2 \phi_4 \phi_8^\dagger + (\phi_2^\dagger)^2 \phi_4^\dagger \phi_8 \right) + \mu_{48} \left((\phi_4)^2 \phi_8^\dagger + (\phi_4^\dagger)^2 \phi_8 \right). \tag{2.1}
\end{aligned}$$

Moving towards symmetry breaking pattern, first the A₄ flavor symmetry is broken by the flavon fields. Then, the spontaneous breaking of B - L gauge symmetry is implemented by assigning non-zero VEV to the scalar singlets ϕ_2 , ϕ_4 and ϕ_8 . Finally, the Higgs doublet breaks the SM gauge symmetry to a low energy theory. The VEV alignment of the scalar fields are denoted as follows.

$$\langle H \rangle = \frac{v}{\sqrt{2}} \begin{pmatrix} 0 \\ 1 \end{pmatrix}, \quad \langle \phi_2 \rangle = \frac{v_2}{\sqrt{2}}, \quad \langle \phi_4 \rangle = \frac{v_4}{\sqrt{2}}, \quad \langle \phi_8 \rangle = \frac{v_8}{\sqrt{2}}, \quad \langle \phi_T \rangle = \frac{v_T}{\sqrt{2}} \begin{pmatrix} 1 \\ 0 \\ 0 \end{pmatrix}, \quad \langle \chi \rangle = \frac{v_\chi}{\sqrt{2}} \begin{pmatrix} 1 \\ 1 \\ 1 \end{pmatrix}.$$

2.2 CP-odd and CP-even scalar mass matrices

The scalar fields $H = (H^+, H^0)^T$ and ϕ_i , ($i = 2, 4, 8$) can be parametrized in terms of real scalars (h_i) and pseudo scalars (A_i) as

$$\begin{aligned}
H^0 &= \frac{1}{\sqrt{2}}(v + h) + \frac{i}{\sqrt{2}}A^0, \\
\phi_i^0 &= \frac{1}{\sqrt{2}}(v_i + h_i) + \frac{i}{\sqrt{2}}A_i, \tag{2.2}
\end{aligned}$$

where v and v_i 's are the corresponding vacuum expectation values. The CP-even component, h of the scalar doublet H , is considered to be the observed Higgs boson at LHC with mass

$M_h = 125$ GeV. We neglect the mixing of Higgs with the new CP-even scalars, h_2 , h_4 and h_8 (corresponding to ϕ_2, ϕ_4 and ϕ_8). The mass matrix in the basis (h_2, h_4, h_8) takes the form

$$M_E^2 = \begin{pmatrix} 2\lambda_{22}v_2^2 & v_2(\sqrt{2}\mu_{24} + \lambda_{24}v_4 + \lambda_{248}v_8) & v_2(\lambda_{248}v_4 + \lambda_{28}v_8) \\ v_2(\sqrt{2}\mu_{24} + \lambda_{24}v_4 + \lambda_{248}v_8) & 2\lambda_4v_4^2 - \frac{v_2^2(\sqrt{2}\mu_{24} + \lambda_{248}v_8)}{2v_4} & \frac{\lambda_{248}v_2^2}{2} + v_4(\sqrt{2}\mu_{48} + \lambda_{48}v_8) \\ v_2(\lambda_{248}v_4 + \lambda_{28}v_8) & \frac{\lambda_{248}v_2^2}{2} + v_4(\sqrt{2}\mu_{48} + \lambda_{48}v_8) & 2\lambda_4v_4^2 - \frac{v_2^2(\sqrt{2}\mu_{24} + \lambda_{248}v_8)}{2v_4} \end{pmatrix}. \quad (2.3)$$

The diagonalization of the above mass matrix results the mass eigenstates, represented by H'_1, H'_2 and H'_3 . Moving to the CP-odd components, A_2, A_4 and A_8 (corresponding to ϕ_2, ϕ_4 and ϕ_8), the mass matrix in the basis (A_2, A_4, A_8) is given by

$$M_O^2 = \begin{pmatrix} -2v_4(\sqrt{2}\mu_{24} + \lambda_{248}v_8) & v_2(\sqrt{2}\mu_{24} - \lambda_{248}v_8) & \lambda_{248}v_2v_4 \\ v_2(\sqrt{2}\mu_{24} - \lambda_{248}v_8) & -\frac{(\sqrt{2}\mu_{24} + \lambda_{248}v_8)v_2^2}{2v_4} - 2\sqrt{2}\mu_{48}v_8 & \frac{\lambda_{248}v_2^2}{2} + \sqrt{2}\mu_{48}v_4 \\ \lambda_{248}v_2v_4 & \frac{\lambda_{248}v_2^2}{2} + \sqrt{2}\mu_{48}v_4 & -\frac{v_4(\lambda_{248}v_2^2 + \sqrt{2}\mu_{48}v_4)}{2v_8} \end{pmatrix}. \quad (2.4)$$

The above mass matrix upon diagonalization, gives one massless eigenstate, to be absorbed by $U(1)$ boson, Z' and two massive modes (represented by A'_1 and A'_2), which remain as massive physical CP-odd scalars in the present framework. The gauge boson Z' attains the mass $M_{Z'} = g_{BL}(4v_2^2 + 16v_4^2 + 64v_8^2)^{1/2}$.

2.3 Lagrangian and Leptonic Mass matrix

The Yukawa interaction Lagrangian for charged leptons, allowed by the symmetries of the model is as follows

$$\begin{aligned} \mathcal{L}_\ell &= -H \left[\frac{y_e}{\Lambda} (\overline{L}_L \phi_T)_1 \otimes e_R + \frac{y_\mu}{\Lambda} (\overline{L}_L \phi_T)_{1'} \otimes \mu_R + \frac{y_\tau}{\Lambda} (\overline{L}_L \phi_T)_{1''} \otimes \tau_R \right] \\ &= -\frac{vv_T}{2\Lambda} \left[y_e(\overline{e}_L e_R) + y_\mu(\overline{\mu}_L \mu_R) + y_\tau(\overline{\tau}_L \tau_R) \right], \end{aligned} \quad (2.5)$$

where, we have used the VEV alignment of the flavon field ϕ_T as discussed in the scalar sector. The Yukawa couplings y_e, y_μ and y_τ are considered to be hierarchical to get the appropriate masses of the charged leptons. The neutral lepton masses are generated by dimension-six operators, from which we derive the Majorana mass term for the neutrinos as

$$\mathcal{L}_\nu = -\frac{y_1}{\Lambda^2} [LLHH]_1 \otimes \phi_2 - \frac{y_\chi}{\Lambda^2} [LLHH]_3 \otimes \chi. \quad (2.6)$$

Out of the three exotic fermions, we consider the fermion with $B - L$ charge 5 to mix with the SM neutrinos, to study the neutrino phenomenology analogous to the mixing between the standard and sterile neutrinos $3 + 1$ mixing scenario. The Majorana mass terms for new fermions and their interaction with SM leptons is given by

$$L_N = -y_{\alpha\beta} \sum_{\alpha, \beta=2,3} (N_\alpha N_\beta \phi_8 + \text{H.c.}) - \frac{y_{11}}{\Lambda} (N_1 N_1 \phi_8^\dagger \phi_2^\dagger + \text{H.c.}) - \frac{y_s}{\Lambda^2} (\overline{L}_H N_1 (\phi_4 \chi)^\dagger + \text{H.c.}). \quad (2.7)$$

The charged lepton mass matrix and 3×3 mass matrix for active neutrinos, obtained from (2.5) and (2.6) respectively, takes the form

$$\mathcal{M}_\ell = \begin{pmatrix} \frac{y_e v v_T}{\Lambda} & 0 & 0 \\ 0 & \frac{y_\mu v v_T}{\Lambda} & 0 \\ 0 & 0 & \frac{y_\tau v v_T}{\Lambda} \end{pmatrix}, \quad \mathcal{M}_\nu = \begin{pmatrix} a + \frac{2d}{3} & -\frac{d}{3} & -\frac{d}{3} \\ -\frac{d}{3} & \frac{2d}{3} & a - \frac{d}{3} \\ -\frac{d}{3} & a - \frac{d}{3} & \frac{2d}{3} \end{pmatrix}. \quad (2.8)$$

Here, $a = \frac{y_1 v_2 v^2}{2\sqrt{2}\Lambda^2}$ and $d = \frac{y_\chi v_\chi v^2}{2\sqrt{2}\Lambda^2}$. The flavor structure of the matrix \mathcal{M}_ν , obtained from A_4 symmetry, can be diagonalized by the TBM mixing matrix [54], given as

$$U_{\text{TBM}} = \begin{pmatrix} -\sqrt{\frac{2}{3}} & \sqrt{\frac{1}{3}} & 0 \\ \sqrt{\frac{1}{6}} & \sqrt{\frac{1}{3}} & -\sqrt{\frac{1}{2}} \\ \sqrt{\frac{1}{6}} & \sqrt{\frac{1}{3}} & \sqrt{\frac{1}{2}} \end{pmatrix}. \quad (2.9)$$

This is for the standard scenario of three neutrinos, that gives a TBM mixing pattern with vanishing reactor mixing angle in the framework of A_4 flavor symmetry, which has been studied in various works in the literature [55–60]. In the next section we consider the active-sterile mixing by introducing an eV scale sterile-like neutrino and discuss the diagonalization of 4×4 neutrino mass matrix.

3 Neutrino mixing with one sterile-like neutrino

The standard scenario of three neutrino species has already been widely discussed in the literature, but the current experimental discrepancies from MiniBooNE and LSND data hint towards the possible existence of the fourth neutrino. From the nomenclature of the sterile neutrinos, one can infer that it doesn't interact with the SM particles directly as it does not have gauge interaction, instead mixes with the active neutrinos during oscillation. The mixing between the flavor (ν_f) and mass eigenstates (ν_i) are related by

$$\nu_f = \sum_{i=1}^n U_i \nu_i, \quad (3.1)$$

where n denotes the number of neutrino species. By considering three generations of active neutrinos, along with n_s number of massive sterile species, one can have $n = 3 + n_s$ dimensional neutrino mixing matrix. In general, the mixing matrix will have $n - 1 = n_s + 2$ Majorana phases, $3 \times (n - 2) = 3 \times (n_s + 1)$ mixing angles and $2n - 5 = 2n_s + 1$ Dirac phases. Hence, in one sterile neutrino scenario, we will have 6 mixing angles, 3 Dirac phases and 3 Majorana phases. The standard parameterization for 4×4 neutrino mixing is given by

$$U = R_{34} \tilde{R}_{24} \tilde{R}_{14} R_{23} \tilde{R}_{13} R_{12} P, \quad (3.2)$$

Table 3: 2σ estimated values of the mixing parameters in one sterile neutrino scenario [9].

	parameter	Δm_{41}^2 [eV]	$ U_{e4} ^2$
3+1/1+3	best-fit	1.78	0.023
	2σ	1.61–2.01	0.006–0.040

where the matrices R_{ij} are rotations in ij space and have the form

$$R_{34} = \begin{pmatrix} 1 & 0 & 0 & 0 \\ 0 & 1 & 0 & 0 \\ 0 & 0 & c_{34} & s_{34} \\ 0 & 0 & -s_{34} & c_{34} \end{pmatrix}, \quad \tilde{R}_{14} = \begin{pmatrix} c_{14} & 0 & 0 & s_{14}e^{-i\delta_{14}} \\ 0 & 1 & 0 & 0 \\ 0 & 0 & 1 & 0 \\ -s_{14}e^{i\delta_{14}} & 0 & 0 & c_{14} \end{pmatrix}, \quad \tilde{R}_{24} = \begin{pmatrix} 1 & 0 & 0 & 0 \\ c_{24} & 0 & 0 & s_{24}e^{-i\delta_{24}} \\ 0 & 0 & 1 & 0 \\ -s_{24}e^{i\delta_{24}} & 0 & 0 & c_{24} \end{pmatrix}. \quad (3.3)$$

Here, $s_{ij} = \sin \theta_{ij}$, $c_{ij} = \cos \theta_{ij}$ and P denotes the diagonal matrix with three Majorana phases α , β and γ ,

$$P = \text{diag} \left(1, e^{i\alpha/2}, e^{i(\beta/2+\delta_{13})}, e^{i(\gamma/2+\delta_{14})} \right). \quad (3.4)$$

The current experimental searches of light sterile neutrino prefer a larger value of active-sterile mass squared differences than the observed solar and atmospheric mass squared differences of active neutrino oscillation. This implies that the mass for sterile neutrino can be either heavier or lighter than the active ones. We know that in normal ordering the active neutrinos have the form $m_3 \gg m_2 > m_1$ whereas the inverse ordering is given by $m_2 > m_1 \gg m_3$. So accordingly, there will be four possibilities in mass orderings if a sterile neutrino is added to the framework. Following the top to bottom nomenclature, i.e. if $m_s \gg m_{1,2,3}$, can be denoted as 1+3 scenario for normal or inverted ordering of the active neutrinos. Whereas, if the case is reversed, i.e. if sterile state is lighter than the active ones ($m_{1,2,3} \gg m_s$), this configuration is named as 3+1 model in literature. Moreover, less attention is given to 3+1 scenario as they are prone to conflict with several experimental observations. In this model, we consider 1+3 like scenarios, to explain the neutrino phenomenology with eV scale exotic fermion.

Table 3 shows the best-fit and 2σ ranges of the relevant oscillation parameters, we used for this work.

3.1 Diagonalization of Neutrino Mass matrix

We assume one of the exotic fermions to be sterile-like to mix with the active neutrinos, is provided by (2.7). We can construct the 4×4 active-sterile mixing matrix for neutrinos as follows

$$\mathcal{M}_\nu = \begin{pmatrix} a + \frac{2d}{3} & -\frac{d}{3} & -\frac{d}{3} & e \\ -\frac{d}{3} & \frac{2d}{3} & a - \frac{d}{3} & e \\ -\frac{d}{3} & a - \frac{d}{3} & \frac{2d}{3} & e \\ e & e & e & m_s \end{pmatrix}, \quad (3.5)$$

where $e = \frac{y_s v v_4 v_\chi}{2\sqrt{2}\Lambda^2}$ and $m_s = \frac{y_{11} v_2 v_8}{2\Lambda}$, are the active-sterile mixing parameter and Majorana mass of the sterile-like fermion respectively. The above mass matrix is analytically diagonalized to get the physical masses of $1 + 3$ neutrinos and the eigenvector matrix is given as

$$U = \begin{pmatrix} \frac{2}{\sqrt{6}} & \frac{1}{6e} \frac{K_-}{N_-} & 0 & \frac{1}{6e} \frac{K_+}{N_+} \\ -\frac{1}{\sqrt{6}} & \frac{1}{6e} \frac{K_-}{N_-} & -\frac{1}{\sqrt{2}} & \frac{1}{6e} \frac{K_+}{N_+} \\ -\frac{1}{\sqrt{6}} & \frac{1}{6e} \frac{K_-}{N_-} & \frac{1}{\sqrt{2}} & \frac{1}{6e} \frac{K_+}{N_+} \\ 0 & \frac{1}{N_-} & 0 & \frac{1}{N_+} \end{pmatrix}, \quad (3.6)$$

where, $K_\pm = a - m_s \pm \sqrt{12e^2 + (a - m_s)^2}$ and $N_\pm^2 = 1 + \frac{(a - m_s \pm \sqrt{12e^2 + (a - m_s)^2})^2}{12e^2}$. If one assumes that $a < m_s$ and expands to second order in the small ratio e/m_s , the resulting mixing matrix is given by [18]

$$U \simeq \begin{pmatrix} \frac{2}{\sqrt{6}} & \frac{1}{\sqrt{3}} & 0 & 0 \\ -\frac{1}{\sqrt{6}} & \frac{1}{\sqrt{3}} & -\frac{1}{\sqrt{2}} & 0 \\ -\frac{1}{\sqrt{6}} & \frac{1}{\sqrt{3}} & \frac{1}{\sqrt{2}} & 0 \\ 0 & 0 & 0 & 1 \end{pmatrix} + \begin{pmatrix} 0 & 0 & 0 & \frac{e}{m_s} \\ 0 & 0 & 0 & \frac{e}{m_s} \\ 0 & 0 & 0 & \frac{e}{m_s} \\ 0 & -\frac{\sqrt{3}e}{m_s} & 0 & 0 \end{pmatrix} + \begin{pmatrix} 0 & -\frac{\sqrt{3}e^2}{2m_s^2} & 0 & 0 \\ 0 & -\frac{\sqrt{3}e^2}{2m_s^2} & 0 & 0 \\ 0 & -\frac{\sqrt{3}e^2}{2m_s^2} & 0 & 0 \\ 0 & 0 & 0 & -\frac{3e^2}{2m_s^2} \end{pmatrix}. \quad (3.7)$$

But this mixing pattern gives $\theta_{13} = 0$, which has already been experimentally ruled out. Hence, to explain the non-zero θ_{13} , we introduce one extra flavon field ζ , which is charged as $1'$ under A_4 symmetry, in order to perturb the neutrino mass matrix from the TBM mixing pattern. Including this new flavon field, the perturbed Lagrangian is given by

$$\mathcal{L}_p = \frac{y_p}{\Lambda^2} [LLHH]_{1''}(\zeta)_{1'} + \text{H.c.} \quad (3.8)$$

When the flavon field acquires VEV, $\langle \zeta \rangle = \frac{1}{\sqrt{2}} \begin{pmatrix} 0 \\ v_\zeta \end{pmatrix}$, the above term contributes to the mass matrix in (3.5). Hence, the modified neutrino mass matrix can be written as

$$\mathcal{M}_\nu = \begin{pmatrix} a + \frac{2d}{3} & -\frac{d}{3} & -\frac{d}{3} & e \\ -\frac{d}{3} & \frac{2d}{3} & a - \frac{d}{3} & e \\ -\frac{d}{3} & a - \frac{d}{3} & \frac{2d}{3} & e \\ e & e & e & m_s \end{pmatrix} + \begin{pmatrix} 0 & 0 & b & 0 \\ 0 & b & 0 & 0 \\ b & 0 & 0 & 0 \\ 0 & 0 & 0 & 0 \end{pmatrix}, \quad (3.9)$$

where, $b = \frac{y_p v^2 v_\zeta}{\Lambda^2}$. We analytically diagonalize the above mass matrix and the mixing matrix is constructed from the normalized eigenvectors, which takes the form

$$U = \begin{pmatrix} \frac{-p_+}{l_{p+}} & \frac{1}{6e} \frac{K_{p-}}{N_{p-}} & \frac{-p_-}{l_{p-}} & \frac{1}{6e} \frac{K_{p+}}{N_{p+}} \\ \frac{q_+}{l_{p+}} & \frac{1}{6e} \frac{K_{p-}}{N_{p-}} & \frac{q_-}{l_{p-}} & \frac{1}{6e} \frac{K_{p+}}{N_{p+}} \\ \frac{1}{l_{p+}} & \frac{1}{6e} \frac{K_{p-}}{N_{p-}} & \frac{1}{l_{p-}} & \frac{1}{6e} \frac{K_{p+}}{N_{p+}} \\ 0 & \frac{1}{N_{p-}} & 0 & \frac{1}{N_{p+}} \end{pmatrix}, \quad (3.10)$$

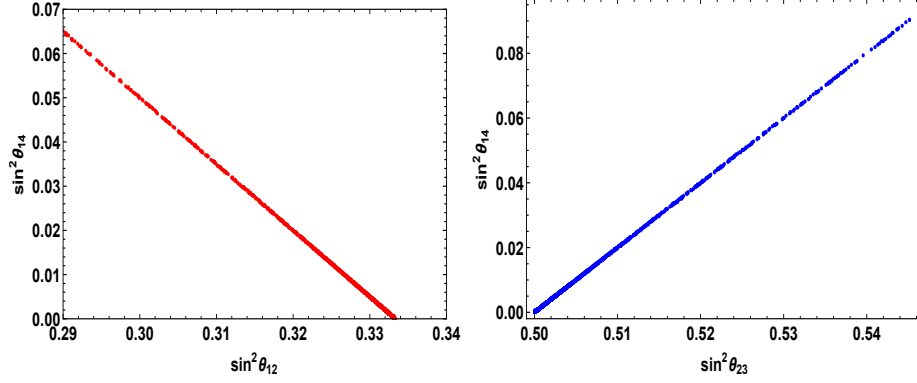


Figure 1: Correlation of the active-sterile mixing angle θ_{14} with solar mixing angle θ_{12} (left panel) and with atmospheric mixing angle θ_{23} (right panel).

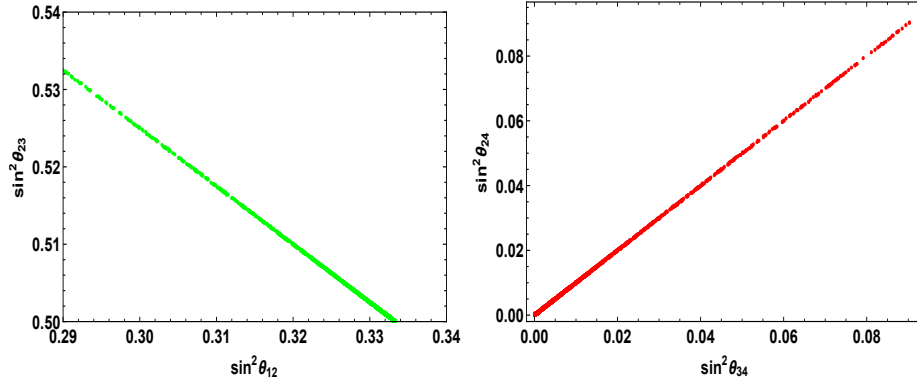


Figure 2: Left panel shows the variation of atmospheric mixing angle θ_{23} and solar mixing angle θ_{12} , right panel represents the variation of active-sterile mixing angles θ_{24} and θ_{34} .

where,

$$\begin{aligned}
K_{p\pm} &= a + b - m_s \pm \sqrt{12e^2 + (a + b - m_s)^2}, \\
N_{p\pm}^2 &= 1 + \frac{\left(a + b - m_s \pm \sqrt{12e^2 + (a + b - m_s)^2}\right)^2}{12e^2}, \\
p_{\pm} &= \frac{a \pm \sqrt{a^2 - ab + b^2}}{a - b}, \quad q_{\pm} = \frac{b \pm \sqrt{a^2 - ab + b^2}}{a - b}, \\
l_{p\pm}^2 &= 1 + (p_{\pm})^2 + (q_{\pm})^2.
\end{aligned} \tag{3.11}$$

And the mass eigenvalues of the 4×4 neutrino mixing matrix are stated as following

$$\begin{aligned}
m_{\nu_1} &= d + \sqrt{a^2 - ab + b^2}, \\
m_{\nu_2} &= \frac{1}{2}[a + b + m_s - \sqrt{12e^2 + (a + b - m_s)^2}], \\
m_{\nu_3} &= d - \sqrt{a^2 - ab + b^2}, \\
m_{\nu_4} &= \frac{1}{2}[a + b + m_s + \sqrt{12e^2 + (a + b - m_s)^2}].
\end{aligned} \tag{3.12}$$

Comparing with the standard 4×4 mixing matrix, we can have the mixing angles as follows

$$\sin^2 \theta_{12} = \frac{|U_{e2}|^2}{1 - |U_{e4}|^2} \simeq \frac{1}{3} \left[1 - 2 \left(\frac{e}{m_s} \right)^2 \right], \quad (3.13)$$

$$\sin^2 \theta_{23} = \frac{|U_{\mu 3}|^2 (1 - |U_{e4}|^2)}{1 - |U_{e4}|^2 - |U_{\mu 4}|^2} \simeq \frac{1}{2} \left[1 + \left(\frac{e}{m_s} \right)^2 \right], \quad (3.14)$$

$$\sin^2 \theta_{14} = |U_{e4}|^2 \approx \left(\frac{e}{m_s} \right)^2, \quad (3.15)$$

$$\sin \theta_{34} = \frac{|U_{\tau 4}|^2}{1 - |U_{e4}|^2 - |U_{\mu 4}|^2} \approx \left(\frac{e}{m_s} \right)^2, \quad (3.16)$$

$$\sin^2 \theta_{24} = \frac{|U_{\mu 4}|^2}{1 - |U_{e4}|^2} \approx \left(\frac{e}{m_s} \right)^2, \quad (3.17)$$

$$\sin^2 \theta_{13} = \frac{|U_{e3}|^2}{(1 - \sin^2 \theta_{23})(1 - \sin^2 \theta_{14})} = \frac{b^2}{4a^2} \left(1 + 2 \frac{e^2}{m_s^2} \right). \quad (3.18)$$

From the above equations, we can infer that adding the perturbation term in the interaction Lagrangian gives non-zero θ_{13} , which is compatible with the current oscillation data.

3.2 Numerical Analysis

To perform numerical analysis in a systematic way, we define $\lambda_1 = \frac{b}{a}$, $\lambda_2 = \frac{d}{a}$ and $\lambda_3 = \frac{e^2}{m_s a}$ with ϕ_{ba} , ϕ_{da} , ϕ_{ea} as the phases of λ_1 , λ_2 and λ_3 respectively. The expressions of mass eigenvalues in (3.19) can thus be written as

$$\begin{aligned} m_{\nu_1} &= |m_{\nu_1}| e^{i\phi_1} = |a| \left| \lambda_2 e^{i\phi_{da}} + \sqrt{1 - \lambda_1 e^{i\phi_{ba}} + \lambda_1^2 e^{2i\phi_{ba}}} \right| e^{i\phi_1}, \\ m_{\nu_2} &= |m_{\nu_2}| e^{i\phi_2} = |a| \left| 1 + \lambda_1 e^{i\phi_{ba}} - 3\lambda_3 e^{i\phi_{ea}} \right| e^{i\phi_2}, \\ m_{\nu_3} &= |m_{\nu_3}| e^{i\phi_3} = |a| \left| \lambda_2 e^{i\phi_{da}} - \sqrt{1 - \lambda_1 e^{i\phi_{ba}} + \lambda_1^2 e^{2i\phi_{ba}}} \right| e^{i\phi_3}, \\ m_{\nu_4} &= |m_{\nu_4}| e^{i\phi_4} = |a| \left| \frac{m_s}{a} + 3\lambda_3 e^{i\phi_{ea}} \right| e^{i\phi_4}. \end{aligned} \quad (3.19)$$

Thus, one obtains the physical masses as

$$\begin{aligned} |m_{\nu_1}| &= |a| \left[(\lambda_2 \cos \phi_{da} + C)^2 + (\lambda_2 \sin \phi_{da} + D)^2 \right]^{\frac{1}{2}}, \\ |m_{\nu_2}| &= |a| \left[(1 + \lambda_1 \cos \phi_{ba} - 3\lambda_3 \cos \phi_{ea})^2 + (\lambda_1 \sin \phi_{ba} - 3\lambda_3 \sin \phi_{ea})^2 \right]^{\frac{1}{2}}, \\ |m_{\nu_3}| &= |a| \left[(\lambda_2 \cos \phi_{da} - C)^2 + (\lambda_2 \sin \phi_{da} - D)^2 \right]^{\frac{1}{2}}, \\ |m_{\nu_4}| &= |a| \left[\left(\frac{m_s}{a} + 3\lambda_3 \cos \phi_{ea} \right)^2 + (3\lambda_3 \sin \phi_{ea})^2 \right]^{\frac{1}{2}}, \end{aligned} \quad (3.20)$$

where,

$$C = \left(\frac{A + \sqrt{A^2 + B^2}}{2} \right)^{\frac{1}{2}}, \quad D = \left(\frac{-A + \sqrt{A^2 + B^2}}{2} \right)^{\frac{1}{2}},$$

$$A = 1 - \lambda_1 \cos \phi_{ba} + \lambda_1^2 \cos 2\phi_{ba}, \quad B = -\lambda_1 \sin \phi_{ba} + \lambda_1^2 \sin 2\phi_{ba}. \quad (3.21)$$

The corresponding phases in the mass eigenvalues values are given by

$$\begin{aligned} \phi_1 &= \tan^{-1} \left[\frac{\lambda_2 \sin \phi_{da} + D}{\lambda_2 \cos \phi_{da} + C} \right], \\ \phi_3 &= \tan^{-1} \left[\frac{\lambda_2 \sin \phi_{da} - D}{\lambda_2 \cos \phi_{da} - C} \right], \\ \phi_2 &= \tan^{-1} \left[\frac{\lambda_1 \sin \phi_{ba} - 3\lambda_3 \sin \phi_{ea}}{1 + \lambda_1 \cos \phi_{ba} - 3\lambda_3 \cos \phi_{ea}} \right], \\ \phi_4 &= \tan^{-1} \left[\frac{3\lambda_3 \sin \phi_{ea}}{\frac{m_s}{a} + 3\lambda_3 \cos \phi_{ea}} \right]. \end{aligned} \quad (3.22)$$

The model also predicts a large CP violating Dirac phase, associated with the non-zero reactor mixing angle, which can be obtained from (3.2)

$$\text{Exp}(-i\delta_{13}) = \frac{U_{13}}{\sin \theta_{13} \cos \theta_{14} \cos \theta_{23}} \approx \text{Exp}(i\phi_{ba}). \quad (3.23)$$

The above equation gives $\sin \delta_{13} \approx -\sin \phi_{ba}$. To constrain the model parameters, compatible with the 3σ limits of the current oscillation data, we perform a random scan of these parameters over the following ranges:

$$\begin{aligned} a &\in [-0.1, 0.1] \text{ eV}, \quad e \in [-0.1, 0.1] \text{ eV}, \quad m_s \in [-1.5, 1.5] \text{ eV}, \quad \lambda_1 \in [0, 0.3], \\ \lambda_2 &\in [0, 1], \quad \lambda_3 \in [0, 0.3], \quad \phi_{ba, da, ea} \in [-\pi, \pi], \end{aligned} \quad (3.24)$$

and show the correlation plots between different mixing angles in Figs. 1 and 2. We now proceed to discuss explicitly the constraints on different parameters from the availed neutrino oscillation data for vanishing and non-vanishing Dirac CP phase, by fixing various model parameters.

3.2.1 Variation of model parameters by fixing $\lambda_2 = 1$ and $\phi_{ba} = 0$

We discuss the dependence of various model parameters, which are consistent with the estimated 3σ values of neutrino oscillation observables. The correlation and constraints on these parameters are presented in Fig. 3 to Fig. 8. Here, we fix $\lambda_2 = 1$ and the phase associated with λ_1 , $\phi_{ba} = 0$. We vary λ_1 and λ_3 from 0 to 0.3 each, which in turn gives a favorable parameter space for λ_1 to lie within 0.25 to 0.3, allowed by the 3σ observation of θ_{13} as shown in the left panel of Fig. 3. From the right panel, the allowed region for λ_3 turns out to be in the range 0.025 to 0.3. We found Majorana like phases ϕ_1 and ϕ_3 to have the allowed values (in radian) of -1.57 to 1.57 (left panel of Fig. 4) and -0.47 to 0.47 (right

Parameter	Best fit $\pm 1\sigma$	2σ range	3σ range
Δm_{21}^2 [10^{-5}eV^2]	7.56 ± 0.19	7.20–7.95	7.05–8.14
$ \Delta m_{31}^2 $ [10^{-3}eV^2] (NO)	2.55 ± 0.04	2.47–2.63	2.43–2.67
$ \Delta m_{31}^2 $ [10^{-3}eV^2] (IO)	$2.47^{+0.04}_{-0.05}$	2.39–2.55	2.34–2.59
$\sin^2 \theta_{12}/10^{-1}$	$3.21^{+0.18}_{-0.16}$	2.89–3.59	2.73–3.79
$\sin^2 \theta_{23}/10^{-1}$ (NO)	$4.30^{+0.20}_{-0.18}$	3.98–4.78 & 5.60–6.17	3.84–6.35
$\sin^2 \theta_{23}/10^{-1}$ (IO)	$5.98^{+0.17}_{-0.15}$	4.09–4.42 & 5.61–6.27	3.89–4.88 & 5.22–6.41
$\sin^2 \theta_{13}/10^{-2}$ (NO)	$2.155^{+0.090}_{-0.075}$	1.98–2.31	1.89–2.39
$\sin^2 \theta_{13}/10^{-2}$ (IO)	$2.155^{+0.076}_{-0.092}$	1.98–2.31	1.90–2.39

Table 4: The experimental values of Neutrino oscillation parameters for 1σ , 2σ and 3σ range [61],[62].

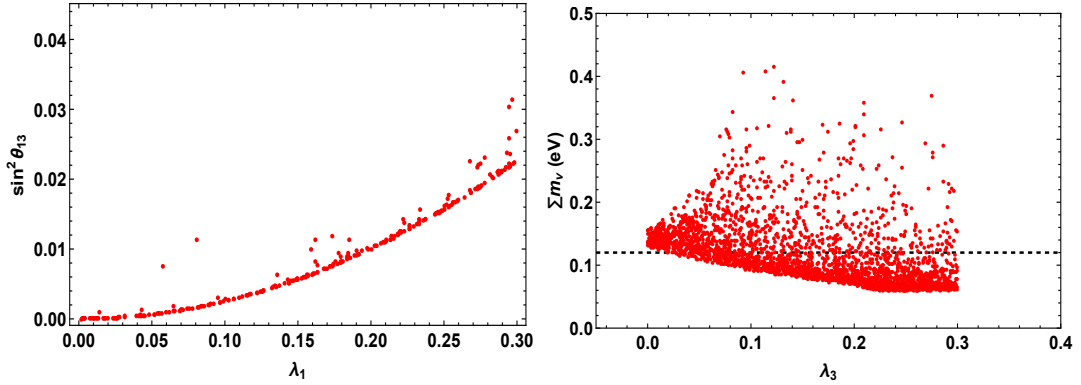


Figure 3: The left panel shows the dependence of the reactor mixing angle θ_{13} on λ_1 and right panel represents the correlation between the sum of total active neutrino masses and λ_3 .

panel of Fig. 4). Similarly, the left panel of Fig. 5 represents a strong constraint on the parameter \mathbf{a} from cosmological observation of total active neutrino mass, which should lie within a range of ± 0.025 to ± 0.035 eV. The right panel displays a correlation between \mathbf{a} and λ_3 . The corresponding phases of λ_2 and λ_3 , i.e ϕ_{da} and ϕ_{ea} are strongly constrained from neutrino mass bound. These phases are found to lie in the range, ± 2.2 to ± 3.14 and -1 to 1.2 radians respectively, as shown in the left and right panels of Fig. 6. The correlation of \mathbf{a} with ϕ_1 and ϕ_{da} are shown in left and right panels of the Fig. 7 respectively. Fig. 8 represents the correlation of ϕ_{da} with ϕ_1 (left panel) and ϕ_3 (right panel). In the present case, by fixing $\phi_{ba} = 0$, one can have a vanishing δ_{13} , even though θ_{13} remains non-zero as seen from Eq.(3.23).

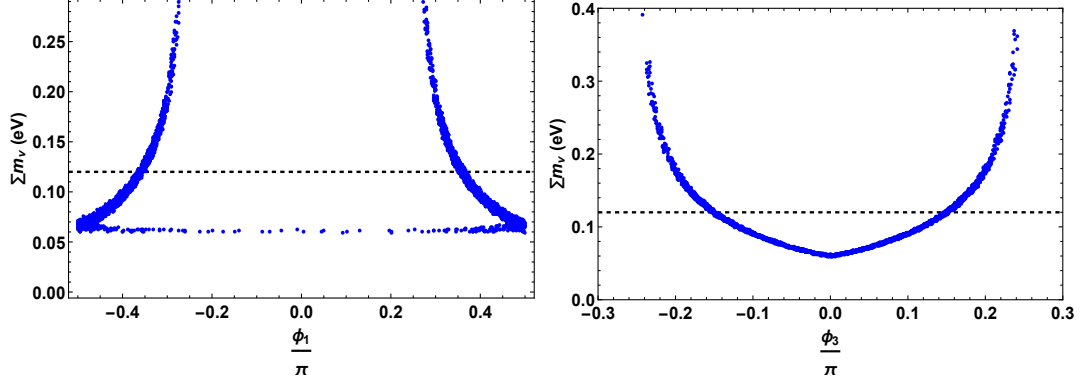


Figure 4: Correlation between the total active neutrino mass with ϕ_1 (left panel) and with ϕ_3 (right panel).

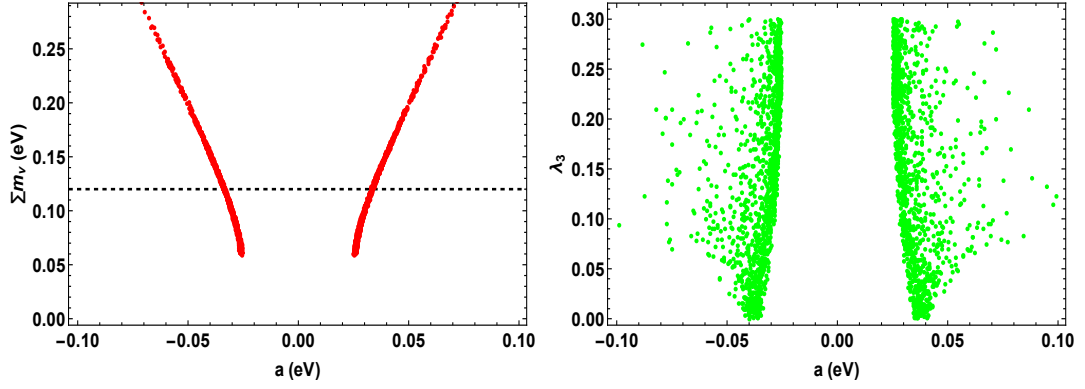


Figure 5: Left panel projects the variation of total active neutrino mass with \mathbf{a} and right panel represents its correlation of λ_3 with \mathbf{a} .

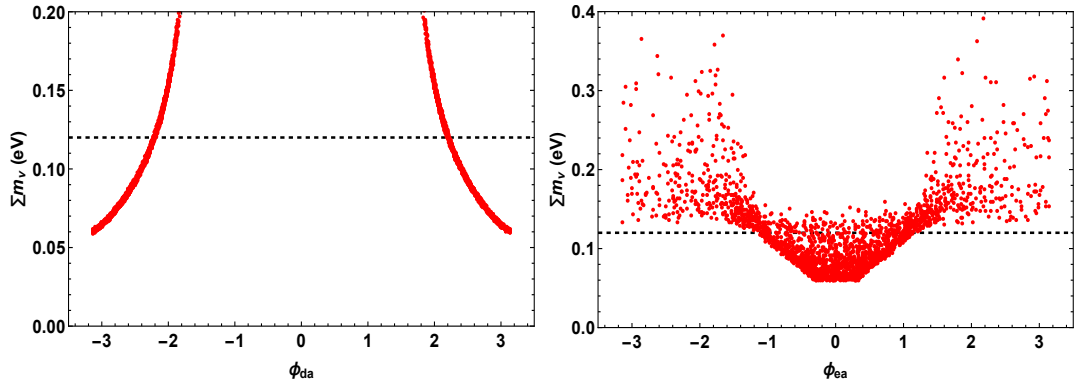


Figure 6: Left (Right) panel shows the variation of total active neutrino masses with ϕ_{da} (ϕ_{ea}).

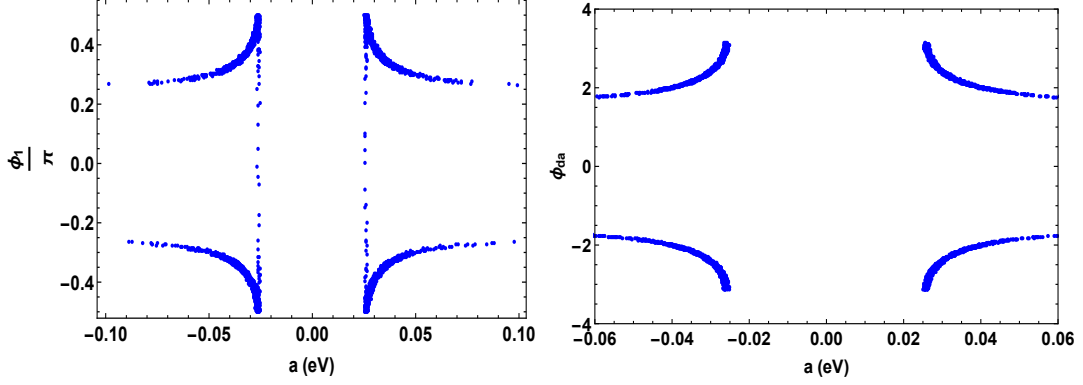


Figure 7: Left (Right) panel represents the variation of ϕ_1 (ϕ_{da}) with \mathbf{a} .

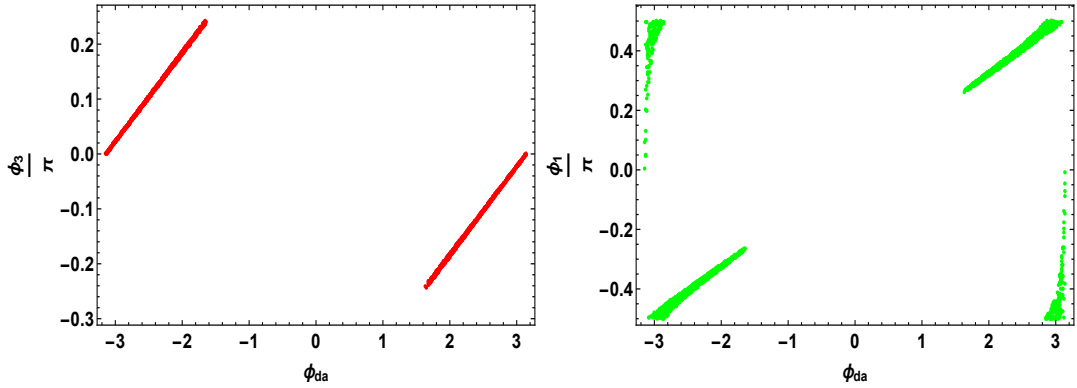


Figure 8: Left panel shows the variation of ϕ_3 with ϕ_{da} and right panel represents the variation of ϕ_1 with ϕ_{da} .

3.2.2 Variation of model parameters by fixing $\lambda_2 = 1$ and $\phi_{ba} \neq 0$

In the previous case, we have a vanishing CP phase ($\delta_{13} = -\phi_{ba}$), here, we try to show the impact of non-zero δ_{13} on the model parameters. We consider the corresponding phase of λ_1 , ϕ_{ba} to vary from $-\pi$ to π , which changes the allowed region of model parameters, described in the previous case. From the left panel of Fig. 9, we found that the region $\lambda_3 > 0.2$ is excluded by the cosmological bound on sum of active neutrino masses. The parameter scan for Majorana like phase allows ϕ_1 (in radian) to lie within the domain 0.94 to 1.2 (first quadrant) and -0.8 to -1 (second quadrant) as shown in the right panel of Fig. 9. The favored parameter space for ϕ_2 and ϕ_3 are represented in Fig. 10, which allows the values of -0.62 to 0.31 for ϕ_2 , 0.25 to 0.62 (first quadrant) and -0.19 to -0.44 (second quadrant) for ϕ_3 (all in radians). In this case, we found that the parameter \mathbf{a} does not change appreciably in comparison with the previous case, as seen from the left panel of Fig. 11. The right panel represents the variation of \mathbf{a} with the CP phase δ_{13} . The correlation of ϕ_1 and ϕ_{da} with parameter \mathbf{a} are shown in the left and right panels of Fig. 12. Fig. 13 project the correlation

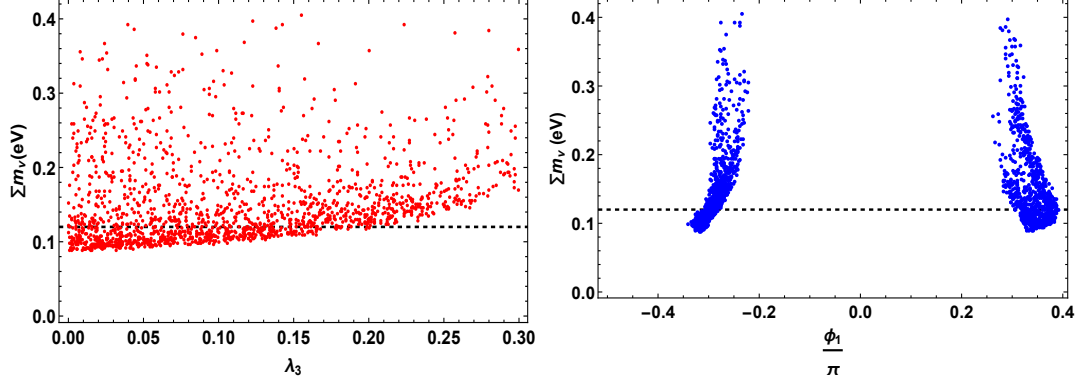


Figure 9: Left (Right) panel shows the variation of total active neutrino masses with λ_3 (ϕ_1).

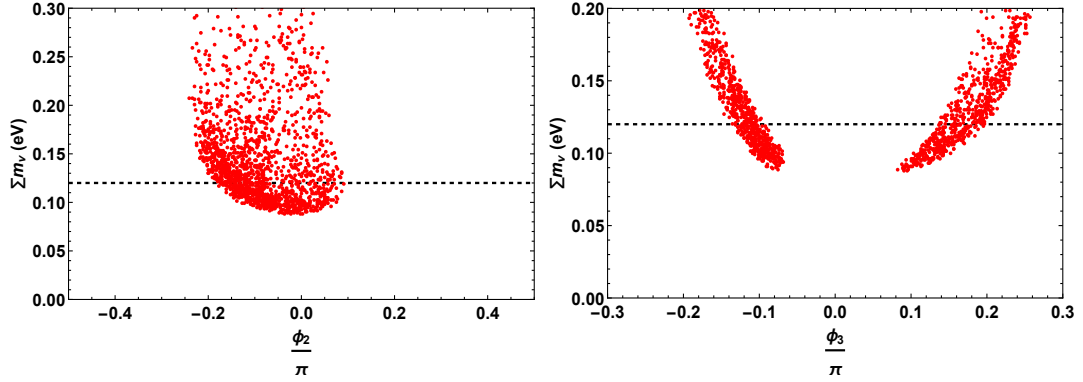


Figure 10: Left (Right) panel shows the variation of total active neutrino masses with ϕ_2 (ϕ_3).

of ϕ_{da} with ϕ_3 (left panel) and ϕ_1 (right panel) respectively.

4 Discussion on neutrinoless double beta decay with eV-scale neutrinos.

To accommodate an eV scale sterile-like neutrino N_1 , with lepton number violating (LNV) Majorana mass manifest the new physics contribution beyond SM. The well known process of NDBD includes the simultaneous decay of two neutrons from the nucleus of an isotope (A, Z) into two protons and two electrons without the emission of any neutrinos in the final state,

$$(A, Z) \rightarrow (A, Z + 2)^{++} + 2e^-.$$

The half-life for a given isotope can be expressed in terms of phase-space factor $\mathcal{G}_{(A,Z)}^{0\nu}$, nuclear matrix element $\mathcal{M}_{(A,Z)}^{0\nu}$ (presented in Table.5) and dimensionless effective parameter

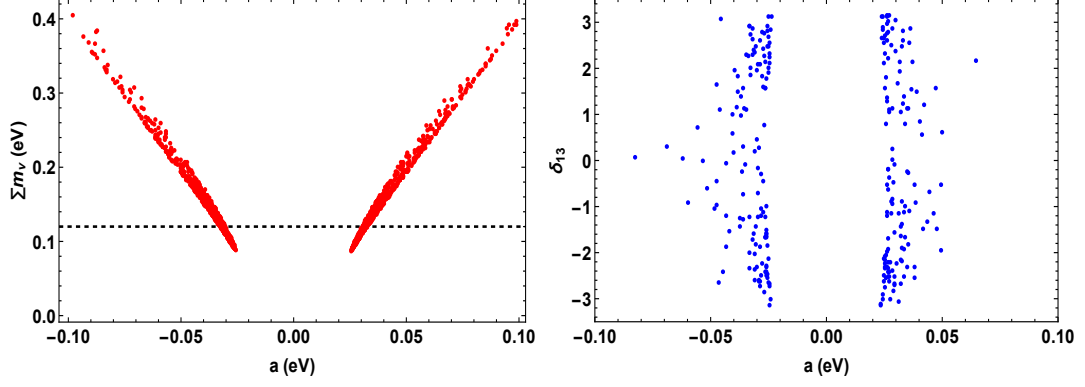


Figure 11: Left panel shows the variation of total active neutrino masses with \mathbf{a} and the right panel depicts the correlation between δ_{13} and \mathbf{a} .

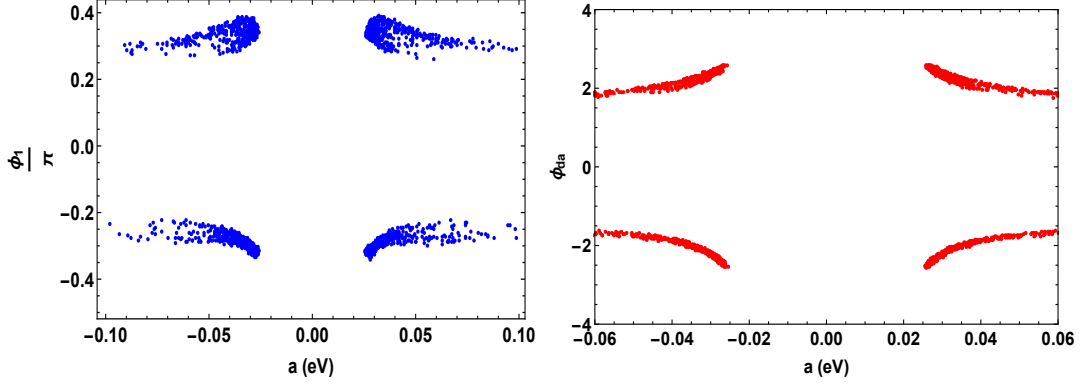


Figure 12: Left (Right) panel shows the variation of ϕ_1 (ϕ_{da}) with \mathbf{a} .

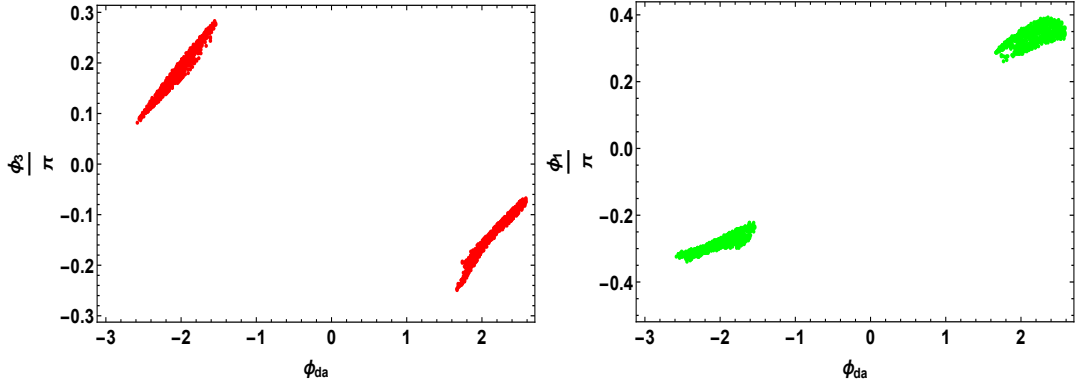


Figure 13: Left (Right) panel shows the variation of ϕ_3 (ϕ_1) with ϕ_{da} .

$\eta_{\text{eff}}^{0\nu}$, which can be inferred from the following expression,

$$(T_{1/2}^{0\nu})_{(A,Z)}^{-1} = \mathcal{G}_{(A,Z)}^{0\nu} |\mathcal{M}_{(A,Z)}^{0\nu} \eta_{\text{eff}}^{0\nu}|^2. \quad (4.1)$$

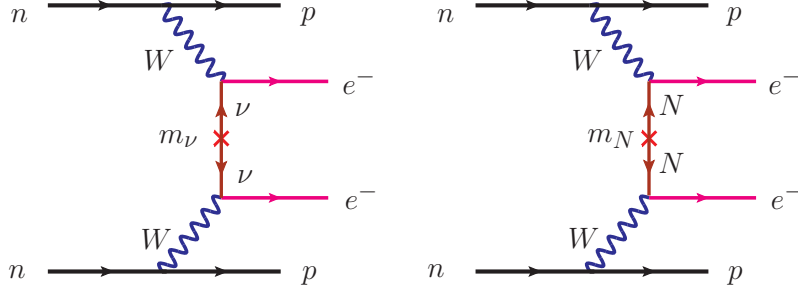


Figure 14: Feynman diagrams contributing to neutrinoless double beta decay with $W^- - W^-$ mediation via the exchange of virtual light neutrinos ν (left panel), and the exchange of virtual eV scale sterile-like neutrinos N (right panel).

Isotope	$G_{0\nu}[10^{-15} \text{ yrs}^{-1}]$	\mathcal{M}_ν
^{76}Ge	7.98	3.85–5.82
^{136}Xe	59.2	2.19–3.36

Table 5: The numerical values of the phase-space factor and nuclear matrix elements

The experimental observation of $0\nu\beta\beta$ process will indicate the existence of an (effective) LNV operator. We discuss here the standard mechanism and new physics contribution to this rare process in the present framework with eV scale sterile-like neutrino.

The process mediated by SM light neutrinos, which are Majorana in nature, is shown in Fig. 14 (left panel). The dimensionless parameter, responsible for LNV is given by the ee element of the Majorana mass matrix, normalized by the electron mass as,

$$\eta_{\text{eff}}^{0\nu} \equiv \frac{m_{ee}^\nu}{m_e} = \frac{1}{m_e} \left(\sum_{i=1}^3 (U_{\text{PMNS}})_{ei}^2 m_i \right). \quad (4.2)$$

where U_{PMNS} is the unitary PMNS mixing matrix and m_i is the mass eigenvalues of the light active neutrinos.

The parametrisation of the PMNS mixing matrix U_{PMNS} is given by

$$U_{\text{PMNS}} = \begin{pmatrix} 1 & 0 & 0 \\ 0 & c_{23} & s_{23} \\ 0 & -s_{23} & c_{23} \end{pmatrix} \begin{pmatrix} c_{13} & 0 & s_{13}e^{-i\delta} \\ 0 & 1 & 0 \\ -s_{13}e^{i\delta} & 0 & c_{13} \end{pmatrix} \begin{pmatrix} c_{12} & s_{12} & 0 \\ -s_{12} & c_{12} & 0 \\ 0 & 0 & 1 \end{pmatrix} \begin{pmatrix} 1 & 0 & 0 \\ 0 & e^{\frac{i\alpha}{2}} & 0 \\ 0 & 0 & e^{\frac{i\beta}{2}} \end{pmatrix} \quad (4.3)$$

where $c_{ij} = \cos \theta_{ij}$, $s_{ij} = \sin \theta_{ij}$ are sine and cosine of the mixing angles, δ is the Dirac CP-phase and α, β are Majorana phases. Using the above mixing matrix U_{PMNS} in eq.(4.2), the modified effective Majorana mass can be read as,

$$m_{ee}^\nu = |m_1 c_{12}^2 c_{13}^2 + m_2 s_{12}^2 c_{13}^2 e^{i\alpha} + m_3 s_{13}^2 e^{i\beta}| \quad (4.4)$$

The effective Majorana mass depends upon the neutrino oscillation parameter θ_{12} , θ_{13} and the neutrino mass eigenvalues m_1 , m_2 and m_3 and phases. However, we do not know the absolute value of these light neutrino masses but neutrino oscillation experiments gives mass square difference between them. Also we have no information about these phases. In our analysis, we randomly vary these phases and took 3σ range of neutrino oscillation parameters to see whether we can get any crucial information about absolute scale of neutrino masses and mass ordering using experimental limit from neutrinoless double beta decay experiments.

We definitely know sign of $\Delta m_{sol}^2 (\equiv \Delta m_{21}^2) = m_2^2 - m_1^2$ is positive which implies $m_2 > m_1$. But neutrino oscillation experiments can not provide unambiguous sign of $m_{atm}^2 (\Delta m_{31}^2)$ which allows two possible ordering of neutrino mass as,

$$\begin{aligned}\Delta m_{atm}^2 (\Delta m_{31}^2) &= m_3^2 - m_1^2, \text{ for Normal Hierarchy (NH)} \\ &= m_1^2 - m_3^2, \text{ for Inverted Hierarchy (IH)}\end{aligned}$$

Normal Hierarchy (NH) : $m_1 < m_2 \ll m_3$

$$\begin{aligned}\text{Here, } m_1 &= m_{\text{lightest}} ; m_2 = \sqrt{m_1^2 + \Delta m_{sol}^2}, \\ m_3 &= \sqrt{m_1^2 + \Delta m_{sol}^2 + \Delta m_{atm}^2}\end{aligned}\tag{4.5}$$

Inverted Hierarchy (IH) : $m_3 \ll m_1 < m_2$

$$\begin{aligned}\text{Here, } m_3 &= m_{\text{lightest}} ; m_1 = \sqrt{m_3^2 + \Delta m_{atm}^2}, \\ m_2 &= \sqrt{m_3^2 + \Delta m_{atm}^2 + \Delta m_{sol}^2}\end{aligned}\tag{4.6}$$

Using these randomly generated input parameters and oscillation data, variations of effective mass with the lightest neutrino mass is displayed in Fig.15. For comparison, we have taken the current experimental limits on the half-life and the corresponding mass parameter for the isotopes ^{76}Ge and ^{136}Xe as follows,

Isotope	$T_{1/2}^{0\nu}$ [10^{25} yrs]	$m_{\text{eff}}^{0\nu}$ [eV]	Collaboration
^{76}Ge	> 2.1	$< (0.2 - 0.4)$	GERDA [63]
^{136}Xe	> 1.6	$< (0.14 - 0.38)$	EXO [64]
^{136}Xe	> 1.9	n/a	KamLAND-Zen [65]
^{136}Xe	> 3.6	$< (0.12 - 0.25)$	EXO + KamLAND-Zen combined [65]

Table 6: The current lower limits on the half-life $T_{1/2}^{0\nu}$ and upper limits on the effective mass parameter $m_{\text{eff}}^{0\nu}$ of neutrinoless double beta decay for the isotopes ^{76}Ge and ^{136}Xe . The range for the effective mass parameter comes from different calculation methods for the nuclear matrix elements.

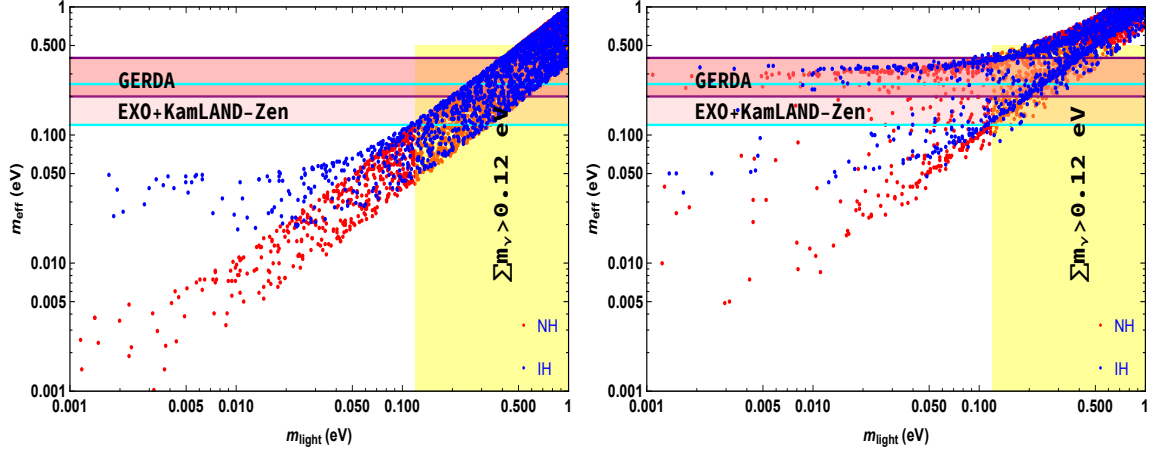


Figure 15: Left Panel: Variation of effective Majorana mass as a function of the lightest neutrino mass, m_1 (m_3) for NH (IH) due to standard mechanism through light active Majorana neutrinos. Right Panel: The new physics contributions (in the presence of eV scale sterile-like neutrino, that falls in the experimental bound discussed in Table 6) to $0\nu\beta\beta$ vs lightest neutrino mass, m_1 (m_3) for NH (IH). The NH contributions are displayed by red dots band while the IH contributions are given by blue dots. The vertical shaded area is for constraint on the sum of light neutrino masses from recent cosmological data (PLANCK1 and PLANCK2). The horizontal shaded areas are for the limits in effective Majorana mass parameter and half-life by GERDA and EXO+KamLAND-Zen experiments.

From left-panel of Fig.15 and using bounds from neutrinoless double beta decay experiments and cosmology, it is quite clear that the standard mechanism is not the only way to realize $0\nu\beta\beta$ and more importantly, NH and IH patterns are insensitive to current experimental bound while the quasi degenerate (QD) pattern is disfavoured from cosmological data from PLANCK1 and PLANCK2. In principle, we should explore all possible sources of new physics that violate lepton number (effectively) by two units and can lead to $0\nu\beta\beta$.

We explicitly found that in addition to the standard mechanism, however, there is an additional contribution coming from the new eV scale sterile-like neutrino. In general the light (ν) and sterile-like (N) neutrino exchange can give the corresponding effective Majorana parameter as

$$m_{ee}^{\text{tot}} = m_{ee}^\nu + m_{ee}^N = \left(\sum_{i=1}^3 U_{ei}^2 m_i + \sum_{i \in \text{eV}} U_{e4}^2 m_{si} \right), \quad (4.7)$$

where U_{e4} is the mixing angle between eV scale sterile neutrino with light active neutrino which has already expressed in terms of model parameters.

The variation of effective Majorana mass parameter in the presence of an additional eV scale sterile neutrino with the lightest neutrino mass is displayed in right-panel of Fig.15. From this plot, we conclude that presence of an additional eV scale sterile-like neutrino

enhances the predictability of the model by contributing to the NDBD (shown in Feynman diagram in Fig. 14). The dotted points which lies in the horizontal bands shows that this new physics contribution can saturate the experimental bounds from GERDA and KAMLAND on effective neutrino mass [66, 67] and can shed light on lepton number violation in nature along-with its implication to cosmology like matter-antimatter asymmetry of the universe.

5 Dark Matter Phenomenology

The model includes two heavy Majorana neutrinos N_2 and N_3 , exotic B – L charges forbid the interaction with SM particles. thereby ensuring the stability. The mixing matrix of these two neutral fermions from (2.7) is given by

$$M_R = \begin{pmatrix} y_{22} \frac{v_8}{\sqrt{2}} & y_{23} \frac{v_8}{\sqrt{2}} \\ y_{23} \frac{v_8}{\sqrt{2}} & y_{33} \frac{v_8}{\sqrt{2}} \end{pmatrix}. \quad (5.1)$$

The above mass matrix can be diagonalized by orthogonal transformation: $U_R M_R U_R^T = M_D$ and the matrix that diagonalize it, is as following

$$U_R = \begin{pmatrix} \cos \theta & \sin \theta \\ -\sin \theta & \cos \theta \end{pmatrix}, \quad M_D = \begin{pmatrix} M_{D_1} & 0 \\ 0 & M_{D_2} \end{pmatrix}. \quad (5.2)$$

Here, the mixing angle is given by $\theta = \frac{1}{2} \tan^{-1} \left[\frac{2y_{23}v_8}{y_{33}v_8 - y_{22}v_8} \right]$.

In the present context, the lightest mass eigenstate obtained from the mixing of N_2 , N_3 qualifies as the dark matter candidate. We use the well-known packages LanHEP [68] and micrOMEGAs [69–71] for the DM analysis. Channels giving significant contribution to relic density are shown in Fig. 16. Annihilation to sterile-like neutrinos ($N_1 N_1$ in final state) in gauge portal and CP-odd scalars ($A'_2 A'_2$ in final state) in scalar portal, stand out to give major contribution. We have fixed the masses of the scalar spectrum and gave emphasis to the impact of gauge parameters $M'_{Z'}$ and g_{BL} on relic density. Fig. 17 left (right) panel depicts the behavior of relic density with DM mass for varying $M_{Z'}(g_{BL})$. Relic density with s-channel contribution is supposed to give resonance in the propagator (Z' , H'_2 , H'_4).

As Z' couples axial vectorially with DM fermion and vectorially with SM fermion, the WIMP-nucleon cross-section is not sensitive to direct detection experiments. Moving to the parameter scan, the gauge parameters $M_{Z'}$ and g_{BL} are restricted from the searches of dilepton signals in Z' -portal by ATLAS [72], and also LEP-II [73]. We have used CalcHEP [74, 75] to obtain the cross section $pp \rightarrow Z' \rightarrow ee(\mu\mu)$ as a function Z' mass, depicted in the left panel of Fig. 18. It can be seen that for $g_{BL} = 0.01$, the region $M_{Z'} < 0.3$ TeV is excluded and for $g_{BL} = 0.03$, the allowed region is $M_{Z'} > 0.9$ TeV. For $g_{BL} = 0.1$, the $M_{Z'}$ should be above 2 TeV. $M_{Z'} > 3$ TeV is allowed for $g_{BL} = 0.3$ and heavy mass regime for Z' (above 4 TeV) is favorable for $g_{BL} = 0.5$. Right panel of Fig. 18 projects the parameter space consistent with Planck relic density limit upto 3σ range, with the exclusion limits of

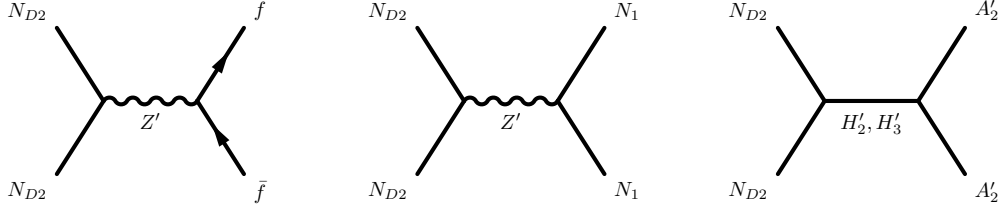


Figure 16: Annihilation channels contributing to relic density.

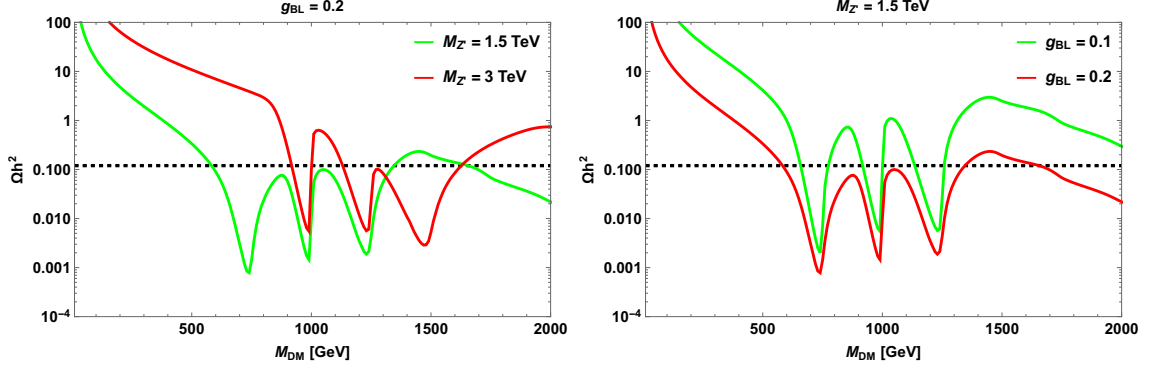


Figure 17: Variation of relic density as a function of DM mass for varying Z' mass (left panel) and g_{BL} (right panel). The benchmark for the masses of the scalars are $(M_{H'_1}, M_{H'_2}, M_{H'_3}, M_{A'_1}, M_{A'_2}) = (2.2, 2, 2.5, 2.1, 0.9)$ (in TeV). Horizontal dashed lines represent 3σ range of Planck limit on relic density.

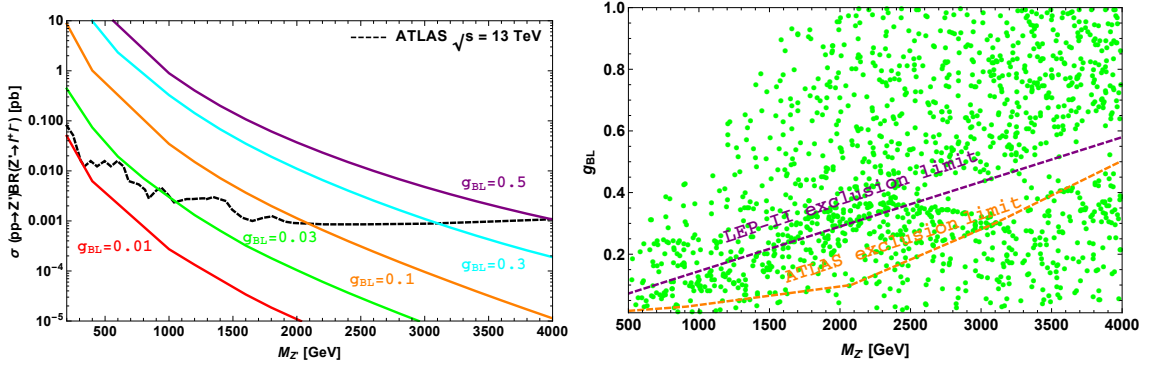


Figure 18: Colored lines in left panel represent the dilepton signal cross section as a function of $M_{Z'}$ for different values of g_{BL} with the black dashed line points to ATLAS bound [72]. Right panel projects the constraint by ATLAS and LEP-II [73] on the gauge parameter space.

ATLAS and LEP-II ($\frac{M_{Z'}}{g_{BL}} > 6.9$ TeV). The favorable region refers to the data points below both the experimental bounds.

6 Summary and Conclusion

In this article, we have presented a detail study of neutrino and dark matter phenomenology in a minimal extension of standard model with $U(1)_{B-L}$ and A_4 flavor symmetry. The model includes additional three neutral fermions with exotic $B - L$ charges of $-4, -4$ and 5 for cancellation of triangle gauge anomalies. The scalar sector is enriched with six SM singlet fields, of them, three are assigned with $U(1)_{B-L}$ charges and the rest three are charged under A_4 flavor symmetry. The former scalar fields helps in spontaneous breaking of $B-L$ symmetry and one massless mode of the CP odd eigenstates gets absorbed by the new gauge boson Z' . The later scalar fields, known as A_4 flavons, break the A_4 flavor symmetry spontaneously at high scale before the breaking of $U(1)_{B-L}$.

As different experiments such as LSND, MiniBooNE etc. are pointing towards the existence of eV scale sterile neutrinos to explain certain experimental discrepancies, we tried to address the neutrino phenomenology with a fourth generation sterile-like neutrino. Out of the three exotic fermions in the model, one is in eV scale (sterile-like) and rest of them are in TeV scale, which help in explaining the neutrino mass and DM simultaneously. The presence of discrete symmetry provides a specific flavor structure to the neutrino mass matrix, leads to a better phenomenological consequences of neutrino mixing with a fourth generation sterile-like neutrino. We explored the active-sterile mixing in compatible with the current experimental observation. We found a large θ_{13} and associated non-zero CP phase, within the observed 3σ range of LSND data by introducing a perturbation term to the Lagrangian. Presence of eV scale sterile-like neutrino also provides an allowed parameter space for the effective neutrino mass in NDBD, lies within the experimental bound of KAMLAND and GERDA. We strongly constrained the model parameters from the cosmological bound of active neutrino masses and showed the correlation between different mixing angles.

Apart from neutrino mixing, we studied the dark matter phenomenology with rest two exotic fermions, by generating the tree level mass in TeV scale unlike the eV scale sterile-like neutrino. By introducing suitable singlet scalar, the mass mechanism for these heavy fermions is assured by the $B - L$ breaking in TeV scale. Within the model framework, we found that the lightest Majorana fermion satisfies correct DM relic density i.e., in the 3σ observation of Planck, with contributions from scalar and gauge mediated processes. As expected, the s-channel resonances for scalars and heavy gauge boson are obtained in the relic density, we have also analyzed the behaviour for different values of model parameters. We also strongly constrained the parameters associated with gauge mediated processes from the ATLAS studies of di-lepton signals and LEP II. We have shown the allowed parameter space satisfying DM and collider constraints. Direct detection of dark matter in Z' portal is insensitive to direct detection experiments because of the Majorana nature. Finally, the proposed idea of extending SM with both gauge and flavor symmetries provides a suitable platform to investigate both neutrino and dark sectors.

7 Acknowledgment

Subhasmita Mishra and Mitesh Kumar Behera would like to acknowledge DST for its financial support. RM acknowledges the support from SERB, Government of India, through grant No. EMR/2017/001448. SM would like to acknowledge Prof. Anjan Giri for his support and useful discussion.

Appendix

A_4 symmetry includes three and one dimensional irreducible representations.

If (a_1, a_2, a_3) and (b_1, b_2, b_3) are the triplets of A_4 , tensor products of these triplets are given as following

$$3 \otimes 3 = 3_s \oplus 3_A \oplus 1 \oplus 1' \oplus 1''$$

$$1 \otimes 1 = 1, \quad 1' \otimes 1'' = 1$$

$$1' \otimes 1' = 1'', \quad 1'' \otimes 1'' = 1'$$

$$\text{Where} \quad 3_s = \begin{pmatrix} 2a_1b_1 - a_2b_3 - a_3b_2 \\ 2a_3b_3 - a_1b_2 - b_1a_2 \\ 2a_2b_2 - a_3b_1 - a_1b_3 \end{pmatrix}, \quad 3_A = \begin{pmatrix} a_2b_3 - a_3b_2 \\ a_1b_2 - a_2b_1 \\ a_3b_1 - a_1b_3 \end{pmatrix}$$

$$1 = a_1b_1 + a_2b_3 + a_3b_2$$

$$1' = a_3b_3 + a_1b_2 + a_2b_1$$

$$1'' = a_2b_2 + a_3b_1 + a_1b_3$$

References

- [1] R. N. Mohapatra and G. Senjanovic, “*Neutrino Mass and Spontaneous Parity Nonconservation*,” *Phys. Rev. Lett.* **44** (1980) 912. [[231\(1979\)](#)].
- [2] S. M. Barr, “*A Different seesaw formula for neutrino masses*,” *Phys. Rev. Lett.* **92** (2004) 101601, [arXiv:hep-ph/0309152](#).
- [3] E. K. Akhmedov and M. Frigerio, “*Interplay of type I and type II seesaw contributions to neutrino mass*,” *JHEP* **01** (2007) 043, [arXiv:hep-ph/0609046](#).
- [4] E. K. Akhmedov, “*Seesaw mechanism and the neutrino mass matrix*,” *Nucl. Phys. Proc. Suppl.* **87** (2000) 321–323, [arXiv:hep-ph/0001041](#). [[321\(1999\)](#)].
- [5] Y. Cai, J. Herrero-Garcia, M. A. Schmidt, A. Vicente, and R. R. Volkas, “*From the trees to the forest: a review of radiative neutrino mass models*,” *Front.in Phys.* **5** (2017) 63, [arXiv:1706.08524](#).

- [6] O. G. Miranda and J. W. F. Valle, “*Neutrino oscillations and the seesaw origin of neutrino mass*,” *Nucl. Phys.* **B908** (2016) 436–455, [arXiv:1602.00864](#).
- [7] O. L. G. Peres and A. Yu. Smirnov, “*(3+1) spectrum of neutrino masses: A Chance for LSND?*,” *Nucl. Phys.* **B599** (2001) 3, [arXiv:hep-ph/0011054](#).
- [8] M. Sorel, J. M. Conrad, and M. Shaevitz, “*A Combined analysis of short baseline neutrino experiments in the (3+1) and (3+2) sterile neutrino oscillation hypotheses*,” *Phys. Rev.* **D70** (2004) 073004, [arXiv:hep-ph/0305255](#).
- [9] J. Kopp, M. Maltoni, and T. Schwetz, “*Are there sterile neutrinos at the eV scale?*,” *Phys. Rev. Lett.* **107** (2011) 091801, [arXiv:1103.4570](#).
- [10] C. Giunti and M. Laveder, “*3+1 and 3+2 Sterile Neutrino Fits*,” *Phys. Rev.* **D84** (2011) 073008, [arXiv:1107.1452](#).
- [11] J. Heeck and W. Rodejohann, “*Sterile neutrino anarchy*,” *Phys. Rev.* **D87** (2013) no. 3, 037301, [arXiv:1211.5295](#).
- [12] **LSND**, A. Aguilar-Arevalo *et al.*, “*Evidence for neutrino oscillations from the observation of anti-neutrino(electron) appearance in a anti-neutrino(muon) beam*,” *Phys. Rev.* **D64** (2001) 112007, [arXiv:hep-ex/0104049](#).
- [13] **Particle Data Group**, M. Tanabashi *et al.*, “*Review of Particle Physics*,” *Phys. Rev.* **D98** (2018) no. 3, 030001.
- [14] **Planck**, N. Aghanim *et al.*, “*Planck 2018 results. VI. Cosmological parameters*,” [arXiv:1807.06209](#).
- [15] C. Blanco, D. Hooper, and P. Machado, “*Constraining Sterile Neutrino Interpretations of the LSND and MiniBooNE Anomalies with Coherent Neutrino Scattering Experiments*,” [arXiv:1901.08094](#).
- [16] **MiniBooNE**, A. A. Aguilar-Arevalo *et al.*, “*Improved Search for $\bar{\nu}_\mu \rightarrow \bar{\nu}_e$ Oscillations in the MiniBooNE Experiment*,” *Phys. Rev. Lett.* **110** (2013) 161801, [arXiv:1303.2588](#).
- [17] M. Dentler, . Hernandez-Cabezudo, J. Kopp, P. A. N. Machado, M. Maltoni, I. Martinez-Soler, and T. Schwetz, “*Updated Global Analysis of Neutrino Oscillations in the Presence of eV-Scale Sterile Neutrinos*,” *JHEP* **08** (2018) 010, [arXiv:1803.10661](#).
- [18] J. Barry, W. Rodejohann, and H. Zhang, “*Light Sterile Neutrinos: Models and Phenomenology*,” *JHEP* **07** (2011) 091, [arXiv:1105.3911](#).
- [19] A. Merle and V. Niro, “*Deriving Models for keV sterile Neutrino Dark Matter with the Froggatt-Nielsen mechanism*,” *JCAP* **1107** (2011) 023, [arXiv:1105.5136](#).
- [20] H. Zhang, “*Light Sterile Neutrino in the Minimal Extended Seesaw*,” *Phys. Lett.* **B714** (2012) 262–266, [arXiv:1110.6838](#).
- [21] P. S. Bhupal Dev and A. Pilaftsis, “*Light and Superlight Sterile Neutrinos in the Minimal Radiative Inverse Seesaw Model*,” *Phys. Rev.* **D87** (2013) no. 5, 053007, [arXiv:1212.3808](#).
- [22] Y. Zhang, X. Ji, and R. N. Mohapatra, “*A Naturally Light Sterile neutrino in an Asymmetric Dark Matter Model*,” *JHEP* **10** (2013) 104, [arXiv:1307.6178](#).

- [23] M. Frank and L. Selbuz, “*Sterile neutrinos in $U(1)$ ’ with R -parity Violation*,” *Phys. Rev.* **D88** (2013) 055003, [arXiv:1308.5243](#).
- [24] R. Adhikari, D. Borah, and E. Ma, “*New $U(1)$ Gauge Model of Radiative Lepton Masses with Sterile Neutrino and Dark Matter*,” *Phys. Lett.* **B755** (2016) 414–417, [arXiv:1512.05491](#).
- [25] N. Nath, M. Ghosh, S. Goswami, and S. Gupta, “*Phenomenological study of extended seesaw model for light sterile neutrino*,” *JHEP* **03** (2017) 075, [arXiv:1610.09090](#).
- [26] P. Das, A. Mukherjee, and M. K. Das, “*Active and sterile neutrino phenomenology with A_4 based minimal extended seesaw*,” *Nucl. Phys.* **B941** (2019) 755–779, [arXiv:1805.09231](#).
- [27] **LUX**, D. S. Akerib *et al.*, “*First results from the LUX dark matter experiment at the Sanford Underground Research Facility*,” *Phys. Rev. Lett.* **112** (2014) 091303, [arXiv:1310.8214](#).
- [28] **XENON100**, E. Aprile *et al.*, “*Dark Matter Results from 225 Live Days of XENON100 Data*,” *Phys. Rev. Lett.* **109** (2012) 181301, [arXiv:1207.5988](#).
- [29] **IceCube**, M. G. Aartsen *et al.*, “*Search for dark matter annihilations in the Sun with the 79-string IceCube detector*,” *Phys. Rev. Lett.* **110** (2013) no. 13, 131302, [arXiv:1212.4097](#).
- [30] **Fermi-LAT**, M. Ackermann *et al.*, “*Search for Gamma-ray Spectral Lines with the Fermi Large Area Telescope and Dark Matter Implications*,” *Phys. Rev.* **D88** (2013) 082002, [arXiv:1305.5597](#).
- [31] **AMS**, M. Aguilar *et al.*, “*First Result from the Alpha Magnetic Spectrometer on the International Space Station: Precision Measurement of the Positron Fraction in Primary Cosmic Rays of 0.5350 GeV*,” *Phys. Rev. Lett.* **110** (2013) 141102.
- [32] **H.E.S.S.**, A. Abramowski *et al.*, “*Search for Photon-Linelike Signatures from Dark Matter Annihilations with H.E.S.S.*,” *Phys. Rev. Lett.* **110** (2013) 041301, [arXiv:1301.1173](#).
- [33] J. Aleksi *et al.*, “*Optimized dark matter searches in deep observations of Segue 1 with MAGIC*,” *JCAP* **1402** (2014) 008, [arXiv:1312.1535](#).
- [34] S. T. Petcov and A. V. Titov, “*The A_4 , S_4 and A_5 flavor symmetries in light of data on neutrino mixing*,” *Int. J. Mod. Phys.* **A33** (2018) no. 31, 1844024.
- [35] E. Ma and G. Rajasekaran, “*Softly broken $A(4)$ symmetry for nearly degenerate neutrino masses*,” *Phys. Rev.* **D64** (2001) 113012, [arXiv:hep-ph/0106291](#).
- [36] G. Altarelli and F. Feruglio, “*Tri-bimaximal neutrino mixing, $A(4)$ and the modular symmetry*,” *Nucl. Phys.* **B741** (2006) 215–235, [arXiv:hep-ph/0512103](#).
- [37] G. Altarelli and D. Meloni, “*A Simplest A_4 Model for Tri-Bimaximal Neutrino Mixing*,” *J. Phys.* **G36** (2009) 085005, [arXiv:0905.0620](#).
- [38] E. Ma, A. Natale, and A. Rashed, “*Scotogenic A_4 Neutrino Model for Nonzero θ_{13} and Large δ_{CP}* ,” *Int. J. Mod. Phys.* **A27** (2012) 1250134, [arXiv:1206.1570](#).
- [39] S. F. King and C. Luhn, “*Neutrino Mass and Mixing with Discrete Symmetry*,” *Rept. Prog. Phys.* **76** (2013) 056201, [arXiv:1301.1340](#).
- [40] M. S. Boucenna, M. Hirsch, S. Morisi, E. Peinado, M. Taoso, and J. W. F. Valle, “*Phenomenology of Dark Matter from A_4 Flavor Symmetry*,” *JHEP* **05** (2011) 037, [arXiv:1101.2874](#).

- [41] D. Meloni, S. Morisi, and E. Peinado, “*Neutrino phenomenology and stable dark matter with A_4* ,” *Phys. Lett.* **B697** (2011) 339–342, [arXiv:1011.1371](#).
- [42] A. Mukherjee and M. K. Das, “*Neutrino phenomenology and scalar Dark Matter with A_4 flavor symmetry in Inverse and type II seesaw*,” *Nucl. Phys.* **B913** (2016) 643–663, [arXiv:1512.02384](#).
- [43] S. Bhattacharya, B. Karmakar, N. Sahu, and A. Sil, “*Unifying the flavor origin of dark matter with leptonic nonzero θ_{13}* ,” *Phys. Rev.* **D93** (2016) no. 11, 115041, [arXiv:1603.04776](#).
- [44] L. M. G. De La Vega, R. Ferro-Hernandez, and E. Peinado, “*Simple A_4 models for dark matter stability with texture zeros*,” *Phys. Rev.* **D99** (2019) no. 5, 055044, [arXiv:1811.10619](#).
- [45] J. C. Montero and V. Pleitez, “*Gauging $U(1)$ symmetries and the number of right-handed neutrinos*,” *Phys. Lett.* **B675** (2009) 64–68, [arXiv:0706.0473](#).
- [46] E. Ma and R. Srivastava, “*Dirac or inverse seesaw neutrino masses with $B - L$ gauge symmetry and S_3 flavor symmetry*,” *Phys. Lett.* **B741** (2015) 217–222, [arXiv:1411.5042](#).
- [47] E. Ma and R. Srivastava, “*Dirac or inverse seesaw neutrino masses from gauged $B - L$ symmetry*,” *Mod. Phys. Lett.* **A30** (2015) no. 26, 1530020, [arXiv:1504.00111](#).
- [48] S. Singirala, R. Mohanta, and S. Patra, “*Singlet scalar Dark matter in $U(1)_{B-L}$ models without right-handed neutrinos*,” [arXiv:1704.01107](#).
- [49] S. Singirala, R. Mohanta, S. Patra, and S. Rao, “*Majorana Dark Matter in a new BL model*,” *JCAP* **1811** (2018) no. 11, 026, [arXiv:1710.05775](#).
- [50] C.-Q. Geng and H. Okada, “*Neutrino masses, dark matter and leptogenesis with $U(1)_{B-L}$ gauge symmetry*,” *Phys. Dark Univ.* **20** (2018) 13–19, [arXiv:1710.09536](#).
- [51] T. Nomura and H. Okada, “*Neutrophilic two Higgs doublet model with dark matter under an alternative $U(1)_{B-L}$ gauge symmetry*,” *Eur. Phys. J.* **C78** (2018) no. 3, 189, [arXiv:1708.08737](#).
- [52] T. Nomura and H. Okada, “*Radiative neutrino mass in an alternative $U(1)_{B-L}$ gauge symmetry*,” *Nucl. Phys.* **B941** (2019) 586–599, [arXiv:1705.08309](#).
- [53] T. Nomura and H. Okada, “*A radiative seesaw model with higher order terms under an alternative $U(1)_{B-L}$* ,” *Phys. Lett.* **B781** (2018) 561–567, [arXiv:1711.05115](#).
- [54] E. Ma, “*Neutrino Tribimaximal Mixing from $A(4)$ Alone*,” *Mod. Phys. Lett.* **A25** (2010) 2215–2221, [arXiv:0908.3165](#).
- [55] N. Memenga, W. Rodejohann, and H. Zhang, “ *A_4 flavor symmetry model for Dirac neutrinos and sizable U_{e3}* ,” *Phys. Rev.* **D87** (2013) no. 5, 053021, [arXiv:1301.2963](#).
- [56] D. Meloni, “*GUT and flavor models for neutrino masses and mixing*,” *Front.in Phys.* **5** (2017) 43, [arXiv:1709.02662](#).
- [57] K. S. Channey and S. Kumar, “*Two simple textures of the magic neutrino mass matrix*,” *J. Phys.* **G46** (2019) no. 1, 015001, [arXiv:1812.10268](#).
- [58] S. K. Garg, “*Consistency of perturbed Tribimaximal, Bimaximal and Democratic mixing with Neutrino mixing data*,” *Nucl. Phys.* **B931** (2018) 469–505, [arXiv:1712.02212](#).

- [59] S. Dev, D. Raj, and R. R. Gautam, “*Deviations in Tribimaximal Mixing From Sterile Neutrino Sector*,” *Nucl. Phys.* **B911** (2016) 744–753, [arXiv:1607.08051](#).
- [60] S. Dev, S. Gupta, and R. R. Gautam, “*Tribimaximal mixing in neutrino mass matrices with texture zeros or vanishing minors*,” *Mod. Phys. Lett.* **A26** (2011) 501–514, [arXiv:1011.5587](#).
- [61] P. F. de Salas, D. V. Forero, C. A. Ternes, M. Tortola, and J. W. F. Valle, “*Status of neutrino oscillations 2018: 3σ hint for normal mass ordering and improved CP sensitivity*,” *Phys. Lett.* **B782** (2018) 633–640, [arXiv:1708.01186](#).
- [62] S. Gariazzo, M. Archidiacono, P. F. de Salas, O. Mena, C. A. Ternes, and M. Trtola, “*Neutrino masses and their ordering: Global Data, Priors and Models*,” *JCAP* **1803** (2018) no. 03, 011, [arXiv:1801.04946](#).
- [63] **GERDA**, M. Agostini *et al.*, “*Results on Neutrinoless Double- β Decay of ^{76}Ge from Phase I of the GERDA Experiment*,” *Phys. Rev. Lett.* **111** (2013) no. 12, 122503, [arXiv:1307.4720](#).
- [64] **EXO-200**, M. Auger *et al.*, “*Search for Neutrinoless Double-Beta Decay in ^{136}Xe with EXO-200*,” *Phys. Rev. Lett.* **109** (2012) 032505, [arXiv:1205.5608](#).
- [65] **KamLAND-Zen**, A. Gando *et al.*, “*Limit on Neutrinoless $\beta\beta$ Decay of ^{136}Xe from the First Phase of KamLAND-Zen and Comparison with the Positive Claim in ^{76}Ge* ,” *Phys. Rev. Lett.* **110** (2013) no. 6, 062502, [arXiv:1211.3863](#).
- [66] P. F. De Salas, S. Gariazzo, O. Mena, C. A. Ternes, and M. Trtola, “*Neutrino Mass Ordering from Oscillations and Beyond: 2018 Status and Future Prospects*,” *Front. Astron. Space Sci.* **5** (2018) 36, [arXiv:1806.11051](#).
- [67] J. T. Penedo and S. T. Petcov, “*The 10^3 eV frontier in neutrinoless double beta decay*,” *Phys. Lett.* **B786** (2018) 410–417, [arXiv:1806.03203](#).
- [68] A. V. Semenov, “*LanHEP: A Package for automatic generation of Feynman rules in gauge models*,” [arXiv:hep-ph/9608488](#).
- [69] A. Pukhov, E. Boos, M. Dubinin, V. Edneral, V. Ilyin, D. Kovalenko, A. Kryukov, V. Savrin, S. Shichanin, and A. Semenov, “*CompHEP: A Package for evaluation of Feynman diagrams and integration over multiparticle phase space*,” [arXiv:hep-ph/9908288](#).
- [70] G. Belanger, F. Boudjema, A. Pukhov, and A. Semenov, “*MicrOMEGAs 2.0: A Program to calculate the relic density of dark matter in a generic model*,” *Comput. Phys. Commun.* **176** (2007) 367–382, [arXiv:hep-ph/0607059](#).
- [71] G. Belanger, F. Boudjema, A. Pukhov, and A. Semenov, “*Dark matter direct detection rate in a generic model with micrOMEGAs 2.2*,” *Comput. Phys. Commun.* **180** (2009) 747–767, [arXiv:0803.2360](#).
- [72] “*Search for new phenomena in the dilepton final state using proton-proton collisions at $\sqrt{s} = 13$ TeV with the ATLAS detector*,” Tech. Rep. ATLAS-CONF-2015-070, CERN, Geneva, Dec, 2015. <https://cds.cern.ch/record/2114842>.
- [73] **DELPHI, OPAL, LEP Electroweak, ALEPH, L3**, S. Schael *et al.*, “*Electroweak Measurements in Electron-Positron Collisions at W-Boson-Pair Energies at LEP*,” *Phys. Rept.* **532** (2013) 119–244, [arXiv:1302.3415](#).

- [74] A. Belyaev, N. D. Christensen, and A. Pukhov, “*CalcHEP 3.4 for collider physics within and beyond the Standard Model*,” *Comput. Phys. Commun.* **184** (2013) 1729–1769, [arXiv:1207.6082](#).
- [75] K. Kong, “*TASI 2011: CalcHEP and PYTHIA Tutorials*,” in *The Dark Secrets of the Terascale: Proceedings, TASI 2011, Boulder, Colorado, USA, Jun 6 - Jul 11, 2011*, pp. 161–198. 2013. [arXiv:1208.0035](#).
<https://inspirehep.net/record/1124593/files/arXiv:1208.0035.pdf>.